CELLULASE AND HEMICELLULASE ACTIVITY WITHIN THE

TIPULA ABDOMINALIS LARVAL GUT

by

THERESA E. ROGERS

(Under the Direction of Joy B. Peterson)

ABSTRACT

In forested stream ecosystems of the north and eastern United States, larvae of the aquatic crane fly *Tipula abdominalis* are important shredders of leaf litter detritus. *T. abdominalis* larvae harbor a dense and diverse microbial community in their hindgut that may aide in the degradation of lignocellulose. In this study, the activities of cellulolytic and hemicellulolytic enzymes were demonstrated from hindgut extracts and from bacterial isolates using model sugar substrates. One of the bacterial isolates was characterized and represents a novel genus, *Crocebacterium* gen, nov., within the family *Microbacteriaceae*, and the type species is *Crocebacterium ilecola* gen, nov., sp. nov. A genomic library of this novel bacterium was constructed to find the genes that encode cellulases and hemicellulases the bacterium produces. A metagenomic library was also constructed in an attempt to find the genes encoding cellulases and hemicellulases from the *T. abdominalis* hindgut community, including as yet uncultivated microorganisms.

INDEX WORDS: *Crocebacterium ilecola, Tipula abdominalis,* lignocellulose degradation, metagenomic library, methylumbelliferone

CELLULASE AND HEMICELLULASE ACTIVITY WITHIN THE *TIPULA ABDOMINALIS* LARVAL GUT

by

THERESA E. ROGERS

B.S., The Ohio State University, 2002

A Thesis Submitted to the Graduate Faculty of the University of Georgia in Partial Fulfillment of the Requirements of the Degree

MASTER OF SCIENCE

ATHENS, GEORGIA

2005

CELLULASE AND HEMICELLULASE ACTIVITY WITHIN THE

TIPULA ABDOMINALIS LARVAL GUT

by

THERESA E. ROGERS

Major Professor:	Joy B. Peterson
Committee:	Eric Stabb William B. Whitman Juergen Wiegel

Electronic Version Approved:

Maureen Grasso
Dean of the Graduate School
The University of Georgia
December 2005

ACKNOWLEDGEMENTS

I would like to thank the members of my committee, Drs. Joy B. Peterson, Eric Stabb, William B. Whitman, and Juergen Wiegel, for their help and advice with the projects written within. I thank my lab members, Dana Cook and Emily DeCrescenzo Henriksen, for their insightful discussions, advice, and support. Thanks are due to Dr. Sue Eggert for her help with larvae collection and Drs. Yong Jin Lee and William B. Whitman for help with various aspects of the characterization of *Crocebacterium ilecola*. I thank Dr. James Travis and his laboratory in the Biochemistry department at the University of Georgia for use of equipment and help with the assays of gut enzyme activity. Thanks are also due to Dr. Jo Handelsman and her laboratory at the University of Wisconsin-Madison, especially Lynn Williamson, for their guidance with metagenomic library construction. I would also like to thank my friends and family for their advice and constant support.

TABLE OF CONTENTS

LIST OF TABLES

Page

LIST OF FIGURES

Page

CHAPTER 1

INTRODUCTION AND LITERATURE REVIEW

Purpose of Study

A delicate balance exists between the input and loss of carbon and energy within stream ecosystems. Carbon and energy enter a stream ecosystem either autotrophically or from terrestrial sources such as fallen leaves and woody debris (Cummins & Klug 1979). A combination of physical, chemical, and biological processes degrade these macromolecular carbon and energy sources. Macroinvertebrate shredders of leaf litter, such as larvae of the aquatic crane fly *Tipula abdominalis*, are major contributors to this degradative process.

T. abdominalis larvae harbor a dense and diverse microbial community in their hindgut. The cooperative activities of *T. abdominalis* larvae and the microbial symbionts residing in its gut to degrade macromolecular carbon and energy sources within stream ecosystems have not been fully established. This study focused on the cellulolytic and hemicellulolytic enzyme activities from gut extracts, microbial isolates, and microorganisms that have yet to be cultivated. First, these enzyme activities were analyzed in gut extracts using sugar substrates conjugated to a compound that fluoresces upon degradation. From these gut extracts, bacteria were isolated and screened on media containing the same fluorescent compound. One of these bacterial isolates, demonstrating enzyme activity on four of the five substrates tested, was then characterized and determined to represent a novel genus within the family *Microbacteriaceae* of the class *Actinobacteria*. Next, a genomic library of this novel bacterium was constructed to determine the source of the cellulolytic and hemicellulolytic activity. Finally, a metagenomic library was

constructed in an attempt to find cellulases and hemicellulases from the entire *T. abdominalis* hindgut community, including uncultivated microorganisms.

In the following sections, the degradation of lignocellulose within steam ecosystems is reviewed. First, the structure of stream ecosystems and the degradation of lignocellulose are discussed. Second, examples are given of interactions between insects and microorganisms that promote the degradation of lignocellulose. Finally, several characteristics of *T. abdominalis* are reviewed, with emphasis on the microbial symbionts residing in the larval gut.

Structure of Stream Ecosystems

Stream ecosystems are classified by their source of energy. Small order, forested streams (orders 0-3) are often shaded from sunlight by trees (Cummins & Klug 1979). Thus, they are highly dependent on terrestrially derived (allochthonous) sources of energy, such as leaves and woody debris that fall into the streams, and are classified as heterotrophic. Larger order streams are wider and have less tree cover, allowing more sunlight to reach the surface. These streams are more dependent on stream-derived (autochthonous) energy sources, such as algae, mosses, and aquatic plants, and are classified as autotrophic. Most streams fall between these two extreme classifications, and are therefore both heterotrophic and autotrophic to varying degrees, depending on the ratio of allochthonous to autochthonous energy input (Cummins & Klug 1979).

All living and non-living organic material in streams regardless of source, such as leaf litter, woody debris, fungi, bacteria, algae, and macroinvertebrates, are collectively called detritus (Cummins & Klug 1979, Maltby 1992). Detritus is best categorized by particle size (Cummins & Klug 1979, Maltby 1992). The four main particle size classifications are coarse particulate organic matter (CPOM) (>1 mm), fine particulate organic matter (FPOM) (<1 mm,

>50 μm), ultrafine particulate organic matter (UPOM) (<50 μm, >0.5 μm), and dissolved organic matter (DOM) (<0.5 μm) (Cummins & Klug 1979). Further divisions occur within each size class, such as course wood (>10 cm) and fine wood (<10cm, >1mm) within the CPOM class (Cummins & Klug 1979).

Energy is derived from the allochthonous organic material in heterotrophic streams by progressive decomposition by leaching, fungi, bacteria, and macroinvertebrates (Cummins & Klug 1979). First, soluble organic matter, such as amino acids, proteins, and sugars, is rapidly leached from the CPOM within 24 hours of falling into the stream, resulting in a loss of 5 – 30 % of the dry weight (Cummins 1974, Petersen & Cummins 1974). Second, aquatic hyphomycete fungi, bacteria, and protozoans colonize the leached CPOM (Suberkropp & Klug 1974). This is often referred to as microbial conditioning. Fungal hyphomycetes are the dominant colonizers of larger, less conditioned allochthonous material and promote the breakdown into smaller particles via enzymes such as cellulases (Cummins & Klug 1979, Suberkropp & Klug 1974). Bacteria are important in the decomposition of particles smaller than 2 - 4 mm since these particles are too small to support fungal hyphal growth (Maltby 1992). Finally, leached and microbially conditioned detritus is then consumed and further macerated by stream macroinvertebrates.

Stream dwelling macroinvertebrates are classified according to feeding strategies (Cummins & Klug 1979). The main four macroinvertebrate classes are shredders, collectors, scrapers, and predators. Shredders mainly consume CPOM, collectors mainly feed on FPOM and UPOM, scrapers consume FPOM while feeding on surface-attached algae, and predators feed mainly on other macroinvertebrates. Essentially all forms of detritus are consumed by all classes of macroinvertebrates, larger size restrictions withstanding. For example, while ingesting CPOM, shredders also consume the more processed forms of detritus: FPOM, UPOM, and DOM

(Cummins & Klug 1979). The feces of these macroinvertebrates are added to the detritus pool, usually as smaller particles than when consumed (Cummins 1974). For example, only about 40% of the CPOM consumed by shredders is assimilated or respired as CO_2, and the rest is added to the FPOM, UPOM, and DOM pools (Cummins 1974).

Degradation of Lignocellulose

After leaching and microbial conditioning, allochthonus material is predominantly composed of lignocellulose (Sinsabaugh et al 1985a, Suberkropp et al 1976). Lignocellulose is a general term for an assemblage of lignin (18-30 %), cellulose (28 – 50 %), and hemicellulose (20 – 30 %) (Breznak & Brune 1994, Enari 1983). Lignin is a non-repetitive structure of various phenylpropanoid subunits (Breznak & Brune 1994). Composition of lignin varies; for example, hardwood lignin consists mainly of guaiacyl- and syringylpropane subunits, whereas softwood lignin consists mainly of guaiacylpropane subunits. Also, grass lignin mainly consists of guaiacyl-, syringyl-, and 4-hydroxyphenylpropane subunits with about 5 – 10 % esterified aromatic acids (Breznak & Brune 1994). Cellulose is an unbranched homopolymer of glucose molecules covalently joined by β-1,4-glycosidic linkages (Enari 1983, Martin 1987b). Hemicellulose is a branched polymer of a variety of sugars, including L-arabinose, D-galactose, D-glucose, D-mannose, D-xylose, and 4-O-methylglucuronic acid (Breznak & Brune 1994, Enari 1983, Martin 1987b, Shallom & Shoham 2003). Hemicellulose composition varies; for example, hemicellulose from hardwood is mainly composed of xylan, whereas hemicellulose from softwood is mainly composed of glucomannan, and arabinogalactans are present in low amounts in both hard- and softwoods (Enari 1983). There are two types of xylan (Martin 1987b). One type, called arabino-4-O-methylglucuronoxylan, is composed of a main chain of xylose with

arabinose and 4-O-methylglucuronic acid in the side chains. The other xylan type is xyloglucan, which is composed of a main chain of glucose with xylose in the side chains. Glucomannans are composed of glucose and mannose in the main chain with galactose in the side chains. Arabinogalactans are composed of galactose in the main chain and arabinose and galactose in the side chains (Martin 1987b). Xylans of grasses are often esterified with phenolic substitutions such as *p*-cumeric acid and ferulic acid (Shallom & Shoham 2003).

Lignin, cellulose, and hemicellulose together form a complex structure (Breznak & Brune 1994, Enari 1983, Martin 1987b). Most cellulose in plants is in highly ordered crystalline bundles called fibrils or microfibrils, which give a plant its rigidity. The cellulose fibrils are surrounded by a matrix of lignin and hemicellulose that are covalently bonded to each other at various intersections. The structural complexity of these polysaccharides increases the recalcitrance of each individual component. For example, cellulases cannot attack cellulose fibrils until the lignin-hemicellulose matrix is broken through (Breznak & Brune 1994, Enari 1983, Martin 1987b).

Hemicellulose is more readily degraded than cellulose and lignin (Breznak & Brune 1994, Martin 1987b). Fungi, bacteria and protozoa produce a variety of enzymes to degrade hemicellulose since it is composed of a variety of sugars (Martin 1987b, Shallom & Shoham 2003). For example, hemicellulose can be degraded by glycoside hydrolases such as arabinase, galactanase, glucanase, mannanase, and xylanase, or carbohydrate esterases, such as ferulic acid esterase, depending on the specific hemicellulose composition (Martin 1987b, Shallom & Shoham 2003). Presence of active hemicellulases can be determined by analyzing the degradation of a variety of *p*-nitrophenyl- or methylumbelliferyl- conjugated sugars, such as *p*-nitrophenyl-α-L-arabinofuranoside and 4-methylumbelliferyl-β-D-mannopyranoside.

Cellulose is less readily degraded than hemicellulose, but more readily degraded than lignin (Breznak & Brune 1994). Cellulase enzymes of the white rot fungi have been extensively studied (Enari 1983, Martin 1987b). White rot fungi produce three major types of cell-free cellulolytic enzymes that all hydrolyze the same β-1,4-glycosidic linkage, but differ by specifically attacking cellulose with different amounts of polymerization or attacking different areas of the macromolecular structure (Martin 1987b). The three enzyme types are endo-β-1,4-glucanases (C_x-cellulases), exo-β-1,4-glucanases (C_1-cellulases), and β-1,4-glucosidases. Endo-β-1,4-glucanases randomly hydrolyze β-1,4-glycosidic linkages, but do not hydrolyze cellobiose. Exo-β-1,4-glucanases attack the non-reducing end of the sugar polymer releasing cellobiose or glucose molecules. Cellobiose and cello-oligosaccharides are hydrolyzed to glucose molecules by β-1,4-glucosidases. Together, these three cellulases can hydrolyze crystalline cellulose and are together referred to as a complete cellulase complex (Martin 1987b). In contrast to fungal cellulases, bacterial cellulases are usually cell-bound; therefore, the bacterial cells require close contact to the substrate in order for degradation to occur (Enari 1983, Martin 1987b). Examples of bacteria that produce cellulases are the actinomycetes, myxobacteria, pseudomonads, and members of the genera *Bacillus*, *Bacteroides, Cellulomonas*, *Clostridium*, and *Ruminococcus* (Enari 1983). Many anaerobic cellulolytic bacteria produce cellulosomes (Bayer et al 2004(Doi, 2003 #155)). These multienzyme complexes are composed of a variety of cellulases and hemicellulases, and may include pectate lyases and chitinases, that are docked on a scaffold attached to the cell surface (Bayer et al 2004(Doi, 2003 #155). The combination of enzymes within the cellulosome act in synergy to degrade lignocellulose more effectively than any of the enzymes alone (Bayer et al 2004, Doi et al 2003).

Presence of active cellulases can be determined by testing the degradation of model substrates (Enari 1983, Martin 1987b). Filter paper, Avicel, cotton, and microcrystalline cellulose are model substrates representing various forms of crystalline cellulose. Carboxymethylcellulose (CMC) and hydroxyethylcellulose (HEC) are common substrates used to demonstrate endo-β-1,4-glucanase activity. Analysis for the production of reducing sugars demonstrates exo-β-1,4-glucanase hydrolysis of the non-reducing ends of Avicel and amorphous cellulose. Supplying the substrates cellobiose, *p*-nitrophenyl-β-D-glucoside or 4-methylumbelliferyl-β-D-glucoside and analyzing for the production of glucose, *p*-nitrophenol or methylumbelliferone, respectively, can demonstrate β-1,4-glucosidase activity (Enari 1983, Martin 1987b).

As detritus is processed and labile compounds decomposed, its lignin composition increases, since lignin is less readily degraded than both hemicellulose and cellulose (Cummins & Klug 1979). The recalcitrance of lignin is attributed to its chemically stable linkages, complex structure, and large size (Breznak & Brune 1994). Various fungi and bacteria, mainly actinomycetes, are capable of hydrolyzing lignin. The white rot fungi and some *Streptomyces* spp. produce extracellular peroxidases to randomly hydrolyze lignin (Breznak & Brune 1994). Also, carboxylesterases may contribute to the degradation of lignin by releasing aromatic esters from the polymeric structure (Breznak & Brune 1994, Sreerama & Veerabhadrappa 1991). Lignin degradation has been studied with the use of ^{14}C-[lignin]-lignocellulose or ^{14}C-labeled synthetic lignins such as dehydrogenative polymerizates (DHPs) (Breznak & Brune 1994).

Insect-Microbe Interactions and the Degradation of Cellulose

The degradation of cellulose by microbial gut symbionts has been described for a small number of insects, while lignin and hemicellulose degradation has been greatly ignored (Breznak & Brune 1994, Delalibera et al 2005, Dillon & Dillon 2004). For this reason, a brief summary of a few examples of insect-microbe interactions is presented in this section, focusing on the degradation of cellulosic material. There are two types of insect-microbe interactions that demonstrate increased degradation of cellulose, both of which involve the use of microbial cellulases. One type is the ingestion of fungi and utilization of the extracellular fungal cellulases to degrade cellulosic rich material. The other type of insect-microbe interaction is the colonization of microorganisms within the alimentary tract that are capable of producing cellulases (Breznak & Brune 1994, Martin 1987b).

One of the most well studied lignocellulose-ingesting insects is the termite. The two classes of termites, lower and higher termites, have dense and diverse microbial communities within their alimentary tracts, and most digest lignocellulose by utilizing these microorganisms in two different manners (Breznak & Brune 1994, Martin 1987b). Lower termites, the families Hodotermitidae, Kalotermitidae, Mastotermitidae, Rhinotermitidae, and Serritermitidae, have cellulose-degrading protozoa residing in the hindgut. Some higher termites, such as the family Termitidae, utilize cellulases produced by ingested fungi to aide in the degradation of lignocellulose (Breznak & Brune 1994, Martin 1987b). For both termite classes, after the lignocellulosic material is degraded to oligo- or monosaccharides, members of the microbial community ferment the sugars to organic acids such as acetate and propionate (Breznak & Brune 1994). These organic acids can then be absorbed through the gut wall and utilized as a source of energy for the termite. Since lignocellulose is a poor source of nitrogen, N_2 fixing microbial gut

symbionts are also important for supplying nitrogen to the termite (Breznak & Brune 1994, Martin 1987b).

Lower termites are capable of producing their own cellulases, yet they will not survive without cellulose-degrading protozoa: oxymonads, trichomonads, and hypermastigote flagellates (Breznak & Brune 1994). The precise reason for this dependence on cellulose-degrading protozoa has not yet been determined. One hypothesis is that the insect-derived cellulases cannot sufficiently hydrolyze cellulose to support termite growth. Another is that the ingested cellulose passes through the gut too quickly without protozoan colonization. Of the higher termites, there exist those that cultivate fungi and those that do not cultivate fungi (Breznak & Brune 1994). The nonfungus-cultivating higher termites, such as *Nasutitermes* sp., produce their own cellulases, and do not appear to rely on microbial-derived cellulase activity for survival. Fungus-cultivating higher termites, such as the subfamily Macrotermitinae, rely on fungal derived cellulases for survival (Breznak & Brune 1994, Martin 1987b). These termites build structures called combs that are made of ingested plant material, slightly digested by rapidly passing through the termite gut. The bastidiomycete *Termitomyces* sp. grows on the comb forming an extensive mycelium and round white nodules of conidiospores. The termites consume both the mycelium and nodules, without which these termites would not survive (Breznak & Brune 1994, Martin 1987b).

Similarly, larvae of siricid woodwasps, such as *Sirex cyaneus* (Hymenoptera, Siricidae), utilize ingested fungal cellulases and amylases to degrade their woody diet (Martin 1987b). Adult female siricid woodwasps harbor fungi, such as *Amylostereum* sp., in two mucus-rich intersegmental pockets. While depositing eggs, the female siricid woodwasp inoculates a tree with the fungi, which colonize the wood surrounding the eggs so the wood is already partially

degraded when the larvae emerge. As the larvae bore through the wood, they spread fungi along the sides of the tunnels allowing for more extensive fungal colonization. Without the fungal symbiont, siricid woodwasp larvae do not survive past the first instar (Martin 1987b).

The contribution of bacterial or fungal derived enzymes capable of degrading lignocellulosic rich material is currently being examined for other insects. For example, cellulose-degrading bacteria have been isolated from the wood borer beetle, *Saperda vestida* (Coleoptera: Cerambycidae), yet any nutritional dependence on these bacteria has not yet been established (Delalibera et al 2005). Low endoglucanase activity in the midgut and hindgut of *T. abdominalis* larvae was attributed to bacterial cellulases (Sinsabaugh et al 1981). In support of this hypothesis, cellulose-degrading bacteria have been recently isolated from the *T. abdominalis* larval hindgut, yet whether their enzymes are active within the gut environment is still unknown (Peterson, unpublished data).

Tipula abdominalis

Larvae of the aquatic crane fly *Tipula abdominalis* (Say) (Diptera; Tipulidae) are major shredders in small order stream ecosystems of the northern and eastern United States (Martin 1987a, Petersen et al 1989) In addition to their great abundance (Martin 1987b), *Tipula* spp. are important to stream ecosystems because they are able to withstand several environmental perturbations. For example, in a resource limitation study of stream ecosystems, abundance and biomass of *Tipula* spp. did not significantly change after three years of leaf litter exclusion (Wallace et al 1999). However, both larval abundance and biomass significantly reduced after woody debris was removed for the fourth year of the same study (Wallace et al 1999). A study focusing on the affects of elevated CO_2-grown leaf litter on bacterial, fungal, and *T. adominalis*

larval growth revealed a large decrease in bacterial production and *T. abdominalis* growth, yet the fungal population seemed unaffected (Tuchman et al. 2002). Leaf litter grown with elevated CO_2 levels had a higher C:N ratio than leaf litter grown under normal CO_2 levels, and was therefore less nutritious for the larvae (Tuchman et al 2002). Although the larvae demonstrated reduced growth, they still persisted in this unfavorable environment. Another study investigated changes in shredder biomass in a first-order stream with elevated levels of chromium, copper, iron, manganese, nickel, lead, and zinc (Woodcock & Huryn 2005). As metal contaminants increased, biomass of shredders such as stoneflies and caddisflies decreased, whereas biomass of *Tipula* spp. remained fairly constant. Since *Tipula* spp. were the most abundant shredders in the stream, regardless of metal contaminants, rates of leaf litter shredding did not significantly change as metal contaminant levels increased (Woodcock & Huryn 2005). This ability to persist in perturbed stream ecosystems when many other shredders perish is one reason *Tipula* spp. are of interest to many stream ecologists.

Tipula spp. have a year-long (univoltine) life cycle. Eggs are laid during warm weather months and are smooth, shiny, black, and oblong in appearance (Pritchard & Hall 1971). Egg size is about 1 mm x 0.4 mm, and there is a long terminal filament at one end that serves to anchor the egg when laid in water (Pritchard & Hall 1971, Tuchman et al 2002). Incubation time before hatching is temperature dependent, with incubation times being shorter in warmer temperatures (Prichard 1983). *Tipula* spp. have four larval instars through which the insect grows and matures, and the transition between instars occurs via ecdysis (molting) (Prichard 1983, Pritchard & Hall 1971). The life cycle of the aquatic crane fly, *Tipula sacra* Alexander, has been well documented (Pritchard & Hall 1971). *T. sacra* larvae of the first instar grow from about 2 to 5 mm long. Larvae of the second and third instars reach lengths of 14 and 20 mm,

respectively. Fourth instar female larvae can grow to 50 mm in length and weigh more than 500 mg, and male larvae can grow to 30 mm in length and weigh more than 300 mg. The larvae then pupate and emerge as adult crane flies that survive only 1 to 5 days, longer lifespans occurring at colder temperatures (Pritchard & Hall 1971). During this short time period as adults, the crane flies mate and the females immediately oviposit on leaf packs or algal mats (Prichard 1983, Pritchard & Hall 1971).

Respiration in well-aerated water occurs both cutaneously and via a pair of spiracles located on the spiracular disc (Pritchard & Hall 1971). Since the size of these spiracles nearly double when molting, but remain the same size between molts, the spiracle diameter measurement is commonly measured to identify the larval instar (Pritchard & Hall 1971). *T. sacra* larvae generally have spiracles larger than 72, 145, and 290 μm for second, third, and fourth instars, respectively (Pritchard & Hall 1971).

Tipulid larvae begin shredding detritus during the first instar and consume the most detritus during the fourth instar (Prichard 1983). Since microorganisms colonize detritus, debates have ensued over whether the microbial biomass or the detritus is the source of larval nutrition (Cummins & Klug 1979, Cummins et al 1973, Golladay et al 1983, Lawson et al 1984, Sinsabaugh et al 1985b). In 1973, Cummins hypothesized that the source of nutrition for shredders is microbial biomass for two reasons. First, leaf detritus is considered an incomplete source of nutrition since its carbon to nitrogen ratio is very high, whereas microbial biomass has a low carbon to nitrogen ratio (Cummins & Klug 1979, Cummins et al 1973). Second, shredders, including *T. abdominalis,* preferentially consume microbially conditioned leaves to those that are unconditioned (Cummins et al 1973, Sinsabaugh et al 1985b).

However, in 1979 Cummins and Klug published results that suggested microbial biomass is not the major source of nutrients for *T. abdominalis*. Of the ingested leaf detritus, 0.03 – 10 % was composed of microbial biomass, and this was estimated to support only 8.3 % of larval growth (Cummins & Klug 1979). Similar results were found by Lawson and colleagues (1984), who estimated that only 11 – 27 % observed *T. abdominalis* larval growth is due to ingested microbial biomass, while the remaining growth is due to ingested leaf material. Also, Golladay and colleagues (1983) demonstrated that shedder growth occurred when either microbially conditioned or unconditioned leaves were consumed. Thus, the majority of *T. abdominalis* larval nutrition is derived from the leaf detritus rather than microbial biomass.

Microorganisms may play a much greater role in *T. abdominalis* nutrition by aiding in the digestion of detritus, as has been observed in other gut systems such as termites and ruminants (Sinsabaugh et al 1985b). Like many other insects, *T. abdominalis* larvae have microbial symbionts residing in its alimentary tract. The *T. abdominalis* larval alimentary tract is composed of a foregut (crop), gastric ceca, midgut (ventricullum), pylorus, ileum, anterior hindgut (rectal lobe), posterior hindgut (rectal sac), and rectum (Klug & Kotarski 1980) (Figure 1.1). The pH of the midgut ranges from 8.5 to 11.6, with the highest alkalinity located in the middle of the midgut, and the hindgut pH range is from 7.1 to 7.5 (Martin 1987b). The midgut and the hindgut harbor a microbial community on the range of 10^8 to 10^{10} cells·mg^{-1}, while the other sections of the alimentary tract are not colonized (Klug & Kotarski 1980). The source of these colonized microbes is believed to be ingested microbially conditioned leaf detritus, since larvae emerging from eggs are not colonized by microorganisms, coprophilic feeding is not observed for aquatic insects, and the microbial community of the midgut lumen is comparable to that found on microbially conditioned leaf detritus (Klug & Kotarski 1980, Lawson et al 1984).

The diversity of the microbial community residing in the *T. abdominalis* larval alimentary tract was studied via microscopy and direct isolation (Klug & Kotarski 1980). Microbial communities were observed in the midgut, anterior hindgut, and posterior hindgut. The midgut lumen consists of a microbial community similar to that found on conditioned leaf detritus with 10^8 cells·mg^{-1}, and the midgut wall not colonized. The hindgut lumen and wall are densely colonized, with 10^9 and 10^{10} cells·mg^{-1}, respectively. The microbial communities associated with the anterior and posterior hindgut lumen and wall are different and more morphologically diverse than the community associated with leaf detritus. The posterior hindgut wall housed the most diverse community overall. The diversity and density of the microbial community increased as the larvae progressed toward the fourth instar. During ecdysis (molting), the hindgut wall splits allowing some of the lumen microbial community to be retained and recolonization of the hindgut wall begins after two days. The predominant morphology within the microbial community is Gram-reaction negative rods, determined by staining techniques. Flagellate and ciliate protozoans are not common inhabitants of the *T. abdominalis* larval gut, and were only found in young or unhealthy larvae. Spores were commonly observed in the gut lumen, however the authors did not determine if they were of fungal or bacterial origin (Klug & Kotarski 1980).

Genetic studies, such as community 16S rRNA gene libraries, are now being analyzed in addition to bacterial enrichments and isolations to study microbial diversity of the *T. abdominalis* hindgut community (Peterson, unpublished). So far, bacteria from the orders *Actinomycetales*, *Coriobacteriales*, *Bacteroidales*, *Deferribacterales*, *Clostridiales*, *Thermoanaerobacteriales*, *Planctomycetales*, *Burkholderiales*, *Enterobacteriales*, *Neisseriales*, *Rhodocyclales*, *Rhodospirillales*, and *Xanthomonadales* have been present in at least one of four 16S rRNA gene

libraries, with a total 322 clones (Cook et al., manuscript in progress). Analysis of the 16S rRNA gene sequences from 59 bacteria isolated from the *T. abdominalis* hindgut revealed high sequence similarity to the genera *Bacillus*, *Caulobacter*, *Georgenia*, *Leifsonia*, *Methylobacterium*, *Microbacterium*, *Micrococcus*, *Paenibacillus*, *Rhodococcus*, *Sanguibacter*, *Serratia*, and *Staphylococcus* (Cook et al., manuscript in progress).

Sinsabaugh and colleagues (1985) hypothesized that microbial symbionts are responsible for the degradation of cellulosic material in the *T. abdominalis* larval gut rather than insect tissue-level synthesized cellulases. It is unlikely that degradation of cellulosic material is due to ingested fungal cellulases since these enzymes would be inactivated by the high pH (~11.0) of the midgut (Martin 1987b, Suberkropp & Klug 1974). Many previous studies had been unsuccessful in detecting significant cellulase activity in the gut of *T. abdominalis* larvae and other aquatic insects (Bjarnov 1972, Martin et al 1981a, Martin et al 1981b, Monk 1976, Sinsabaugh et al 1985a). Using carboxymethylcellulose (CMC) as a substrate, Sinsabaugh and colleagues (1985) successfully demonstrated low endoglucanase activity in the midgut and hindgut of *T. abdominalis*, but were unable to demonstrate exoglucanase activity. In a study involving radiolabeled cellulose, Sinsabaugh and colleagues (1985) demonstrated the assimilation of purified cellulose, which was converted to organic and amino acids presumably by microbial symbionts before transport across the gut wall.

Objectives

Objective 1. To demonstrate cellulolytic and hemicellulolytic activity from fresh *T. abdominalis* gut extracts at a physiologically relevant pH. *T. abdominalis* midgut and hindgut extracts were analyzed for cellulolytic and hemicellulolytic enzyme activities using sugar substrates conjugated to methylumbelliferone, a compound that fluoresces upon release from the sugar. The natural pH of the *T. abdominalis* midgut is about 11.0; therefore the enzyme assays of midgut extracts were performed at this alkaline pH. Likewise, the enzyme assays of hindgut extracts were performed at pH 7.4 since this is the typical pH of the *T. abdominalis* hindgut. To reduce loss of enzyme activities, the gut extracts were prepared the day of analysis.

Objective 2. To culture novel bacteria as well as bacteria previously isolated from the *T. abdominalis* larval hindgut. These bacterial isolates were screened for degradative enzyme activity on methylumbelliferyl-conjugated substrates. Bacteria repeatedly isolated from the *T. abdominalis* larval gut were fully characterized.

Objective 3. To discover novel cellulases and hemicellulases from the microbial symbionts of the *T. abdominalis* hindgut. Genomic libraries from novel bacterial isolates and metagenomic libraries of whole gut homogenates were constructed and screened for cellulolytic and hemicellulolytic enzyme activities. The screen utilized media containing methyumbelliferyl-conjugated substrates.

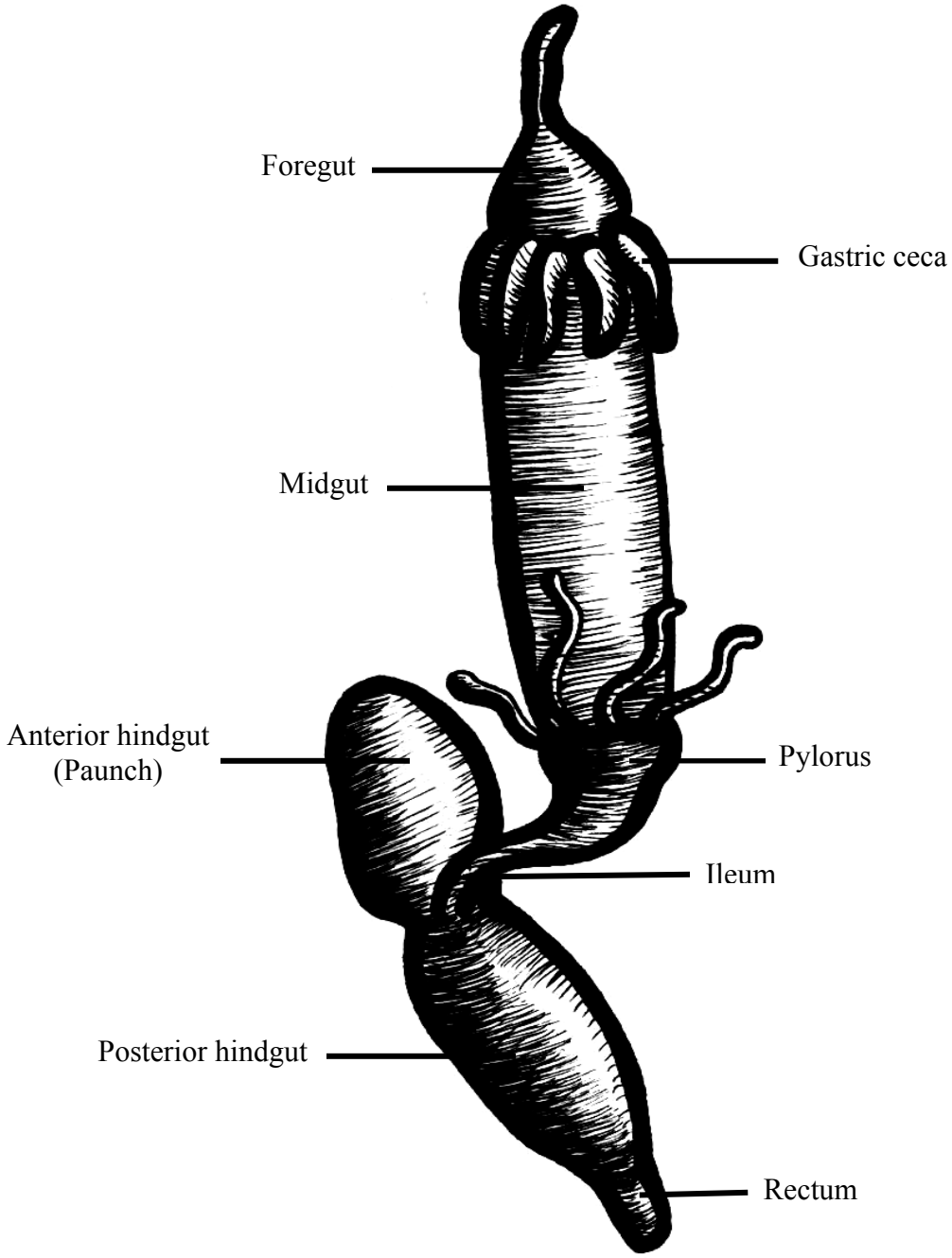

Figure 1.1. *Tipula abdominalis* alimentary tract. Figure is redrawn from Klug and Kotarski, 1980. Figure is not drawn to scale.

CHAPTER 2

ANALYSIS OF CELLULOLYTIC AND HEMICELLULOLYTIC ENZYME ACTIVITY WITHIN THE *TIPULA ABDOMINALIS* GUT

Introduction

Sinsabaugh and colleagues (1985) successfully demonstrated exoglucanase activity within the hindgut of *T. abdominalis* using carboxymethyl cellulose (CMC) as a substrate. In their study, reducing assays were performed on gut extracts buffered to a pH of 6.0, a pH lower than that found in either the midgut or the hindgut. Also, gut extracts were not assayed the day of dissection; rather they were stored at 4 °C until assayed, introducing a potential loss of enzyme activity (Sinsabaugh et al 1985b).

Because *T. abdominalis* larvae assimilated purified cellulose, which was converted to organic and amino acids before transport across the gut wall, degradation of cellulosic material must occur within the alimentary tract (Sinsabaugh et al 1985b). This study aimed to demonstrate the activity of cellulolytic and hemicellulolytic enzymes within the *T. abdominalis* larval gut. The midgut and hindgut of *T. abdominalis* were separated in order to assay their activities at a physiologically relevant pH values of 11.0 and 7.4, respectively (Martin et al 1980b). Although the high pH in the midgut is generally associated with proteolytic activity (Graca & Barlocher 1998, Martin et al 1980b) and inactivation of fungal cellulases (Barlocher & Porter 1986, Martin et al 1980b, Sinsabaugh et al 1985a, Suberkropp et al 1976), alkaline cellulases from bacterial soil isolates have been described previously (Singh et al 2004). It was

therefore necessary to measure cellulolytic and hemicellulolytic activity within the midgut at pH 11.0.

Methylumbelliferyl- (MU-) conjugated sugars were the substrates used in these assays, because previous studies of the bacterial isolates from *T. abdominalis* hindgut homogenates demonstrated activity on MU-conjugated sugars (Peterson, unpublished). MU-conjugated substrates have also been used to demonstrate the activity of extracellular enzymes in marine systems, the digestive tracts of freshwater snails, and of the larvae of two Trichoptera species (Brendelberger 1997, Hoppe 1983, Schulte et al 2003). Cleavage of the MU-conjugated substrate liberates the fluorescent compound methylumbelliferone, which allows for measurement of substrate degradation (Hoppe 1983). Although MU- conjugated sugars are not long-chain polymers, they competitively inhibit degradation of naturally occurring disaccharides (Hoppe 1983). The MU-conjugated sugars resemble sugar polymer ends and oligosaccharides produced by degradation of the larger polymeric sugars. The cleavage of MU- substrates therefore indicates the potential for polymer degradation.

Methods

Collection Site

Fourth instar *T. abdominalis* larvae were collected from Shope Fork Creek, Coweeta, NC. Stream parameters were as follows: pH 5.35; dissolved oxygen, 11.2 mg L^{-1}; water temperature, 7.7 ˚C; conductivity, 14.58 µs cm^{-1}; turbidity, 0.47 NTU; alkalinity, 12.0 mg L^{-1}; <1 mg L^{-1} NO_3^-; and <0.1 mg L^{-1} PO_4^{3-}. Larvae were stored at 12 ºC in an aerated 4 L container filled with filter-sterilized stream water and leaves collected from the stream of capture. Water was

changed every three to four days. Of the twelve larvae, four per day were dissected and their gut homogenates were assayed 14, 23, and 28 days after their capture.

Larval Dissection

T. abdominalis larval midguts (with foregut attached) and hindguts were removed and separated during dissection under $BSS_{7.4}$ buffer, pH 7.4 (10.8 mM K_2HPO_4, 6.9 mM KH_2PO_4, 21.5 mM KCl, 24.5 mM NaCl, 1.0 mM DTT) (Leadbetter & Breznak 1996) (Figure 1.1). Midguts were placed in 5 ml BSS_{11} buffer, pH 11.0 (25 mM Na_2CO_3, 24.5 mM KCl, 1.0 mM DTT), and hindguts were placed in 5 ml $BSS_{7.4}$ buffer, pH 7.4.

Sample Preparation

Protocol was modified from Schulte, et al. (2003) and Brendelberger (1997). Midguts and hindguts were sonicated in a Branson 1510 ultrasonic bath (Branson Ultrasonics, Danbury, Conn.) for 1 min, then centrifuged at 3,500 x g and 4˚C for 30 min (Schulte et al 2003). The supernatant was removed and placed into a new tube, and from here on in is called the "enzyme extract." The centrifuged gut pellet was resuspended in buffer of appropriate pH and from here on in is called the "resuspended gut extract." From both the enzyme extract and resuspended gut extract, a 1 ml aliquot was filtered through a 0.2 μm filter to screen for cell-free enzyme activity; "filtered enzyme extract" and "filtered resuspended gut extract." Another 1ml aliquot was boiled for 30 min to serve as a negative control; "boiled enzyme extract" and "boiled resuspended gut extract" (Schulte et al 2003). To determine if controls were free of viable microorganisms, 200-μl aliquots of the filtered and boiled extracts were spread-plated onto tryptic soy agar (TSA, DIFCO) and compared to plates spread with enzyme extracts and resuspended gut extracts,

described below. All gut extracts were assayed on the day of dissection. A previously studied bacterial isolate from the *T. abdominalis* gut (isolate 27, accession number AY504453) known to demonstrate activity on all MU-substrates in this study was used as a positive control. The unfiltered gut extracts represent microorganisms residing within the gut lumen and those that were easily dislodged from the gut wall. The resuspended gut extracts represent the microorganisms attached to the gut wall, and the filtered gut extracts represent cell-free enzymes.

Preparation of Stock Solutions and Standards

Stock solutions of the MU- standard and substrates were prepared by dissolving in 5 ml of 70% (v/v) ethanol, then diluting to 50 ml with autoclaved distilled water to a final concentration of 2 mM. Standard concentrations of methylumbelliferone sodium salt (Sigma) were 100.0, 50.0, 25.0, 20.0, 15.0, 10.0, and 1.0 μM (Schulte et al 2003). New standards were prepared daily since fluorescence diminished upon storage at –20 ºC. The five MU- conjugated sugars used as model substrates were 4-methylumbelliferyl-α-L-arabinofuranoside (MUA, Sigma), 4-methylumbelliferyl-β-D-cellobioside (MUC, Sigma), 4-methylumbelliferyl-β-D-glucopyranoside (MUG, Sigma), 4-methylumbelliferyl-β-D-mannopyranoside (MUM, Sigma), and 4-methylumbelliferyl-β-D-xyloside (MUX, Sigma) (Figure 2.1). In contrast to the methylumbelliferone sodium salt standard, the methylumbelliferyl-conjugated substrate solutions were stable upon storage at –20 ºC.

Enzyme Assay

Enzyme activity was assayed in black 350 μl 96-well plates (NUNC) with a spectrofluorometer Spectra MAX® GEMINI EM, Molecular Devices. Unfiltered, filtered, and

boiled enzyme extracts and resuspended gut extracts (40 µl) were mixed with BSS buffer, pH 11.0 for midgut and 7.4 for hindgut (155 µl), and MU- substrate (5 µl). Top read, endpoint fluorescence enzyme assays began with substrate addition and were incubated for 20 to 30 min at 25 ˚C. Fluorescence was measured at 360 nm emission and 435 nm excitation with no cutoff wavelength, and values were the average of twenty readings (Schulte et al 2003). Fluorescence values directly relate to liberated methylumbelliferone concentrations.

Isolation, Screening, and Identification of Bacteria from the Hindgut

Hindgut and resuspended gut extracts of two larvae were plated onto TSA and Luria-Bertani agar (LBA, DIFCO) media in 50 and 75 µl aliquots and incubated at room temperature until no new colonies appeared (after nine days). A total of 198 colonies were streaked onto additional TSA or LBA plates for isolation. Colonies were picked according to morphology and incubation time before colony appearance to reduce repetition of isolates, picking only three to four colonies with similar morphology if found on different plates or from different gut extracts. Glycerol stocks of 40 % (w/v) glycerol were made of each bacterial isolate for storage at –80 ˚C. Isolates were then screened on TSA + 1 $g \cdot L^{-1}$ MUA, MUC, MUG, MUM, or MUX by replica plating. Isolates were allowed to grow for one full week before plates were checked for fluorescence under a UV lamp.

Ten of these isolates had similar morphology and incubation time before colony appearance to isolate C3 (accession number AY497196; Peterson, unpublished data), a bacterium previously isolated from the hindgut of *T. abdominalis* larvae from North Carolina and Michigan. Sequencing of the partial 16S rRNA gene was performed by MIDI Labs (Newark, DE). Partial 16S rRNA genes were PCR amplified with primers corresponding to *E. coli*

positions 005 and 531. Sequences with high similarity to the partial 16S rRNA genes of the ten isolates were obtained from a BLAST search with GenBank (http://www.ncbi.nlm.nih.gov).

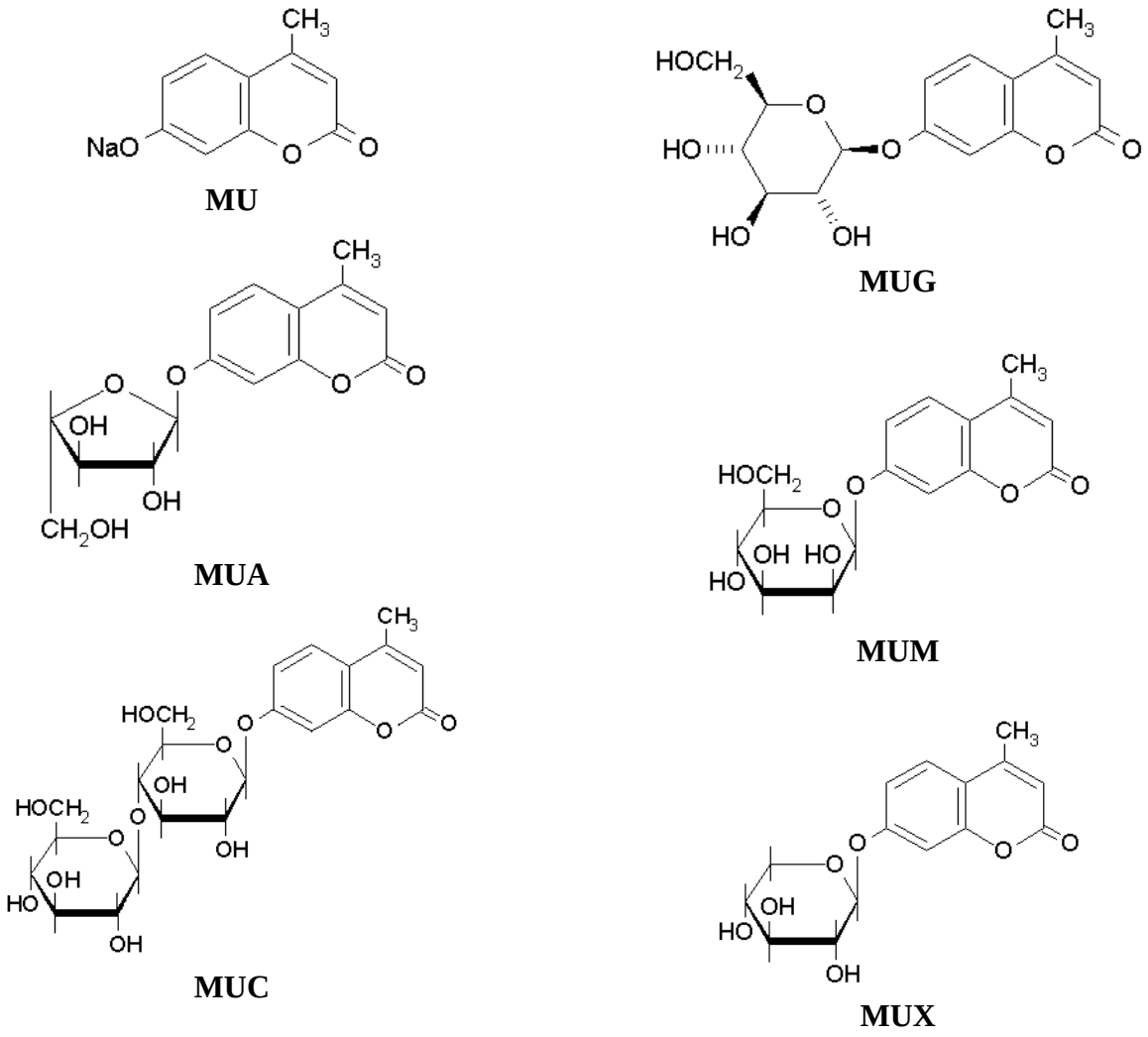

Figure 2.1. Methylumbelliferone and methylumbelliferyl-conjugated sugars. Abbreviations are as follows: methylumbelliferone, MU; 4-methylumbelliferyl-α-L-arabinofuranoside, MUA; 4-methylumbelliferyl-β-D-cellobioside, MUC; 4-methylumbelliferyl-β-D-glucopyranoside, MUG; 4-methylumbelliferyl-β-D-mannopyranoside, MUM; and 4-methylumbelliferyl-β-D-xyloside, MUX. Figures are from GFS Chemicals Product Catalog (http://gfschemicals.com/).

Results

Enzyme Assay

All five substrates were hydrolyzed by the unfiltered and filtered hindgut enzyme extracts (Figures 2.2 and 2.3). However, hydrolysis of MUG was up to 13 times greater than hydrolysis of the other four MU-conjugated sugars by hindgut enzyme extracts. Both unfiltered and filtered resuspended hindgut extracts hydrolyzed MUG, MUA, and MUX, while only unfiltered resuspended hindgut extracts hydrolyzed MUC significantly more than the negative controls (Figures 2.2 and 2.3). Activity of unfiltered and filtered resuspended hindgut extracts on MUM was similar to negative controls (Figure 2.3). All unfiltered and filtered midgut enzyme extracts and resuspended midgut extracts had similar activity to the negative controls (Figure 2.4). No bacterial colonies formed on TSA plates inoculated with filtered and boiled extracts. All enzyme extracts and resuspended gut extracts were assayed the day of dissection since significant enzyme activity was lost when frozen at –20 ºC overnight and reassayed the following day.

Isolation, Screening, and Identification of Bacteria from the Hindgut

Of the 198 isolates, 35.3, 39.4, 58.1, 27.3, and 35.9 % displayed activity on MUA, MUC, MUG, MUM, and MUX, respectively (Table 2.1). These numbers roughly resemble the relative hindgut enzyme extract activity on each of the five MU-conjugated sugar substrates (Figures 2.2 and 2.3). For example, enzyme activity was highest with MUG and lowest with MUM. Also, the degradation of MUA, MUC, and MUX were similar.

A

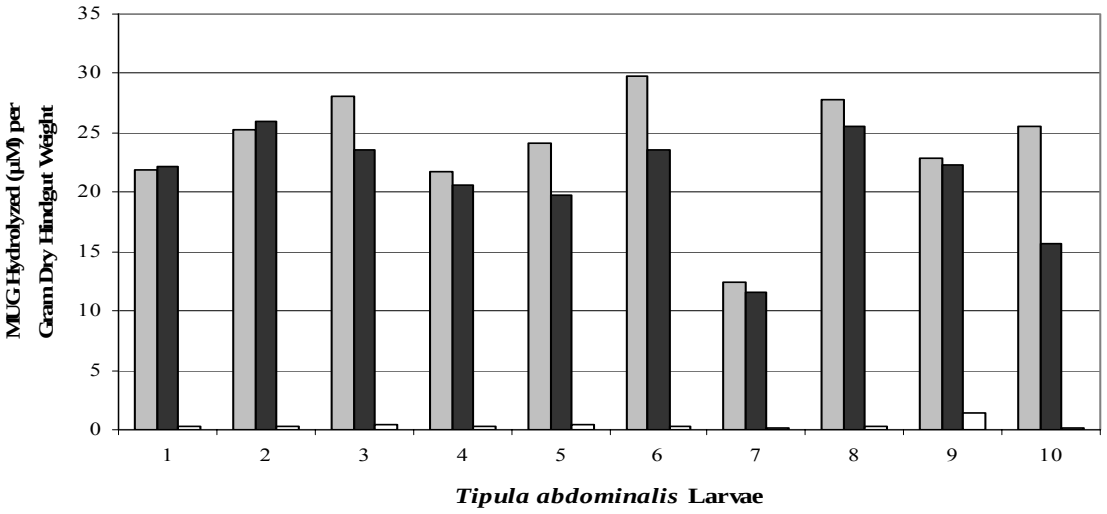

B

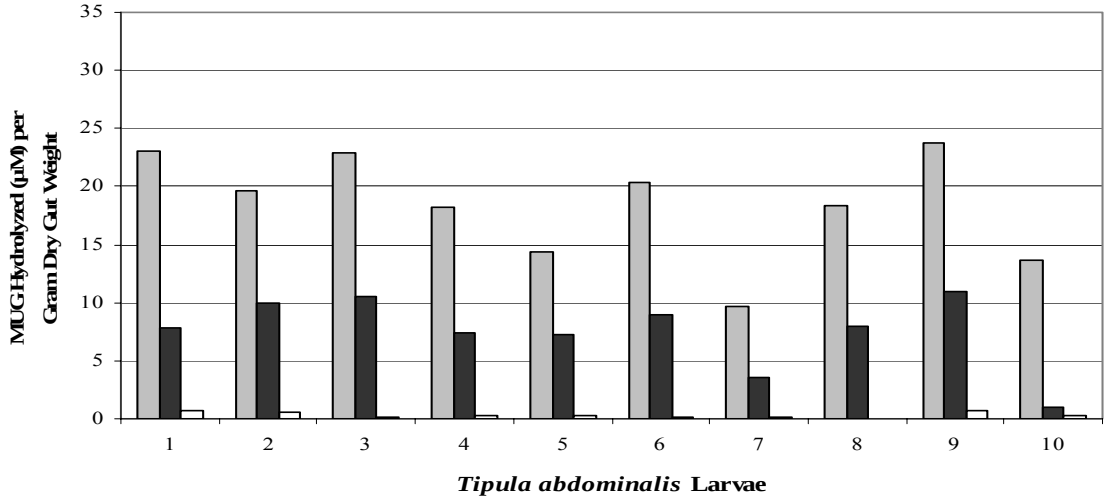

Figure 2.2. MUG hydrolyzed (µM·g^{-1} dry gut weight) by ten individual *Tipula abdominalis* larvae hindgut enzyme extracts and resuspended guts. Hindgut enzyme extracts and resuspended guts are presented as unfiltered (grey), filtered (black), and boiled (white). (A) Hindgut enzyme extracts from animals 1 and 2, 3-6, and 7-10 were assayed 14, 23, and 28 days after capture, respectively. (B) Resuspended guts from animals1-3, 4-6, and 7-10 were assayed 14, 23, and 28 days following capture, respectively. All assays were performed between 20 and 30 minutes.

A

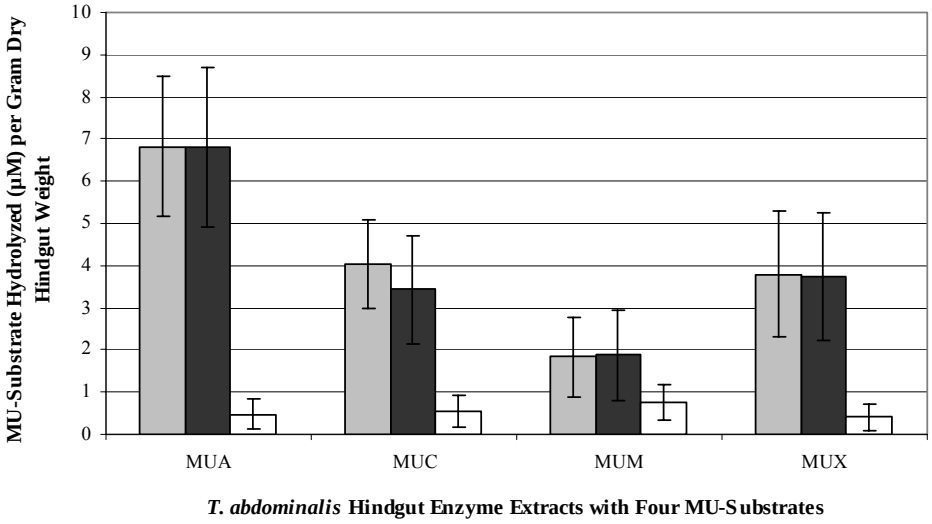

B

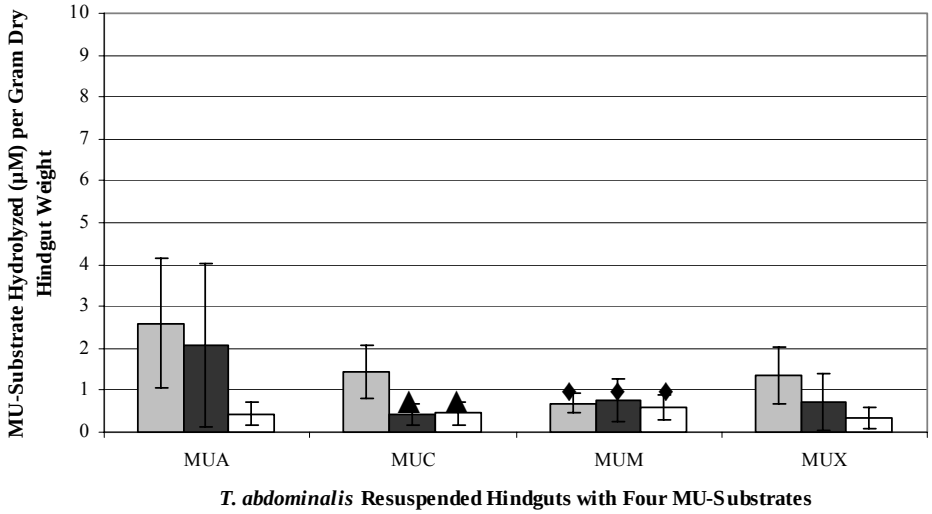

Figure 2.3. Average *Tipula abdominalis* hindgut enzyme extract and resuspended hindgut activity (µM·g^{-1} dry gut weight) on four MU- substrates. Hindgut enzyme extracts and resuspended guts are presented as unfiltered (grey), filtered (black), and boiled (white). Data are for ten animals. All unfiltered and filtered enzyme extracts and resuspended guts are significantly different ($P \leq 0.001$), determined by student T tests, from boiled enzyme extracts except unfiltered resuspended gut activity on MUM (♦) and filtered resuspended gut activity on MUC (▲) and MUM (♦). All assays were performed between 20 and 30 minutes.

A

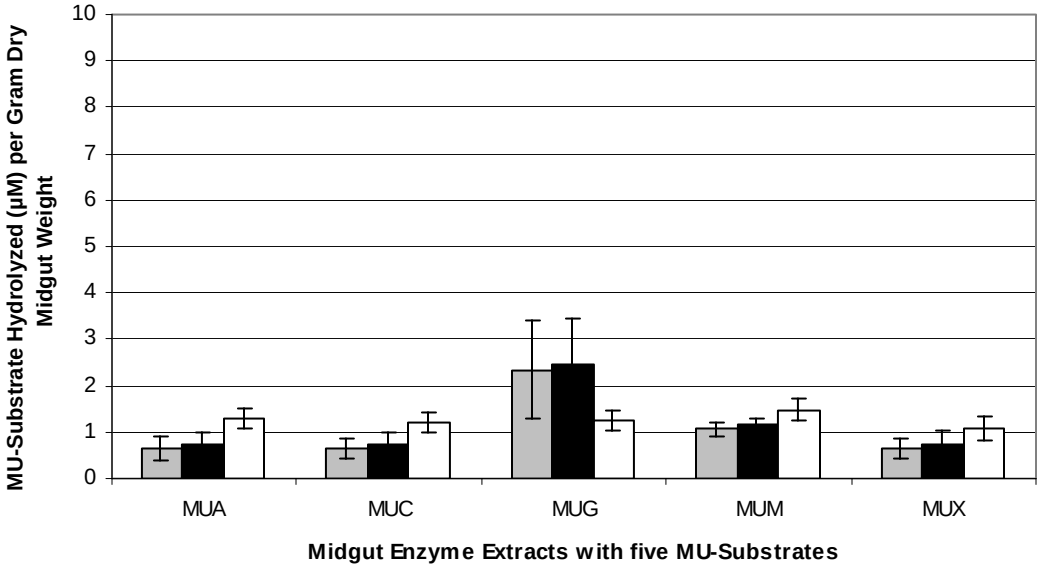

B

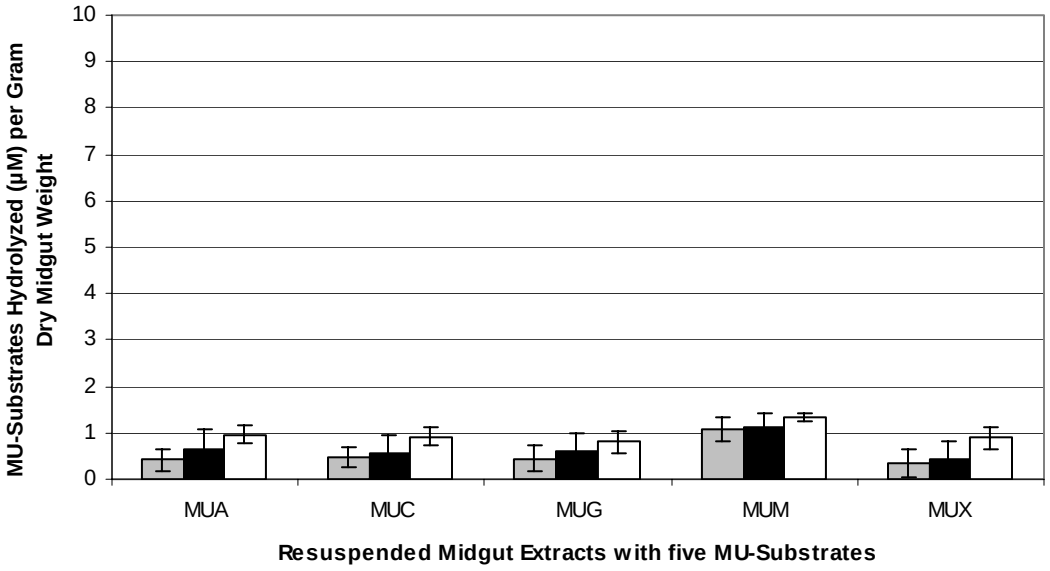

Figure 2.4. Average *Tipula abdominalis* midgut enzyme extract and resuspended midgut activity (µM·g^{-1} dry gut weight) on five MU- substrates. Midgut enzyme extracts and resuspended midguts are presented as unfiltered (grey), filtered (black), and boiled (white). Data are for ten animals. All assays were performed between 20 and 30 minutes.

Colonies plated from hindgut and resuspended hindgut extracts began appearing on the media overnight and continued to appear through nine days (Table 2.1). Many colony morphologies were observed. Of colony colors, white, cream, pale and bright yellow, pale, bright and dark orange, pinkish orange, and dark purple were observed. Many colony shapes and textures were also observed including round, irregular, smooth, wrinkled, concave, convex, and drop-like (Table 2.1).

Table 2.1. Colony morphology, incubation time before colony appearance, and degradative enzyme activity on media containing MU-conjugated substrates for isolates T21 – T219.

Isolate	Colony Morphology*	Growth[†]	MUA[‡]	MUC	MUG	MUM	MUX
T21	W, small, round, shiny, convex, smooth	36 h	-	-	-	-	-
T22	C, small, round, shiny, convex, smooth	36 h	-	-	-	-	-
T23	O-Y, small, round, shiny, convex, smooth	36 h	+	+	+	-	+
T24	O-Y small, round, shiny, convex, smooth	36 h	+	+	+	-	-
T25	C, small, irregular edge, wrinkled, concave	24 h	-	-	+	-	-
T26	W, small, round, shiny, convex, smooth	5 d	+	-	+	-	+
T27	C, small, round, fuzzy	5 d	-	-	-	-	-
T28	W, small, round, shiny, convex, smooth	5 d	-	-	+	-	-
T29	W, small, round, shiny, convex, smooth	48 h	+	-	-	-	-
T30	Y, tiny, round, smooth, shiny, drop-like	9 d	-	-	-	-	-
T31	Bright O, small, round, shiny, convex, smooth	48 h	-	-	-	-	-
T32	O, small, round, shiny, convex, smooth	36 h	-	-	-	-	-
T33	Light O, small, round, shiny, convex, smooth	36 h	-	-	-	-	-
T34$^{\infty}$	Dark Y, small, round, shiny, convex, smooth	48 h	+	-	-	-	-
T35$^{\infty}$	Y, small, round, shiny, convex, smooth	5 d	+	+	+	-	-
T36	O-Y, small, round, shiny, convex, smooth	36 h	+	+	+	-	-
T37	Pale O-Y, small, round, shiny, convex, smooth	36 h	+	+	+	-	-
T38	Pale Y, small, round, shiny, convex, smooth	36 h	-	-	+^{w}	-	-
T39$^{\infty}$	Dark Y, small, round, shiny, convex, smooth	48 h	+	-	-	-	-
T40	W, small, round, shiny, convex, smooth	5 d	+	-	+	-	+^{w}
T41$^{\infty}$	Dark Y, small, round, shiny, convex, smooth	48 h	+	+	-	-	-
T42	O-Y, small, round, shiny, convex, smooth	36 h	+	+	+	+	+
T43	O-Y, small, round, shiny, convex, smooth	36 h	+	+	+	+	+
T44	Y, small, round, shiny, convex, smooth	36 h	+	+	+	+	+
T45	Pale C, very small, round, shiny, smooth, convex	nd[§]	-	-	-	-	-
T46	C, small, round, shiny, convex, smooth	5 d	-	-	-	-	-
T47	C, small, round, shiny, convex, smooth	36 h	+	+	+	+	+
T48	Pale Y, shiny, round, entire, small, raised	24 h	-	+^{w}	+	-	-

T49	C with W middle, round, shiny, convex, smooth	48 h	-	-	-	-	-
T50	C, flat, filamentous, spreading	16 h	-	-	-	-	-
T51	C, round, scalloped margin, convex	16 h	-	+[w]	+	-	-
T52	Pale C, small, round, shiny, crateriform, smooth	36 h	+	+	+	+	+
T53	C, small, round, shiny, convex, smooth	5 d	-	+	+	-	-
T54	W, small, round, shiny, convex, smooth	5 d	+	+	-	-	-
T55	W, small, round, shiny, convex, smooth	5 d	+	-	+	-	+
T56	W, small, round, shiny, convex, smooth	5 d	+	-	+	+	-
T57	C, small, round, shiny, convex, smooth	5 d	-	-	+	+	-
T58	Pale Y, round, shiny, convex, smooth	16 h	-	-	-	-	-
T59	C, small, round, shiny, convex, smooth	5 d	-	-	-	-	-
T60	Pale C, small, round, shiny, convex, smooth	36 h	+	+	+	+	+
T61	Pale C, small, round, shiny, convex, smooth	5 d	+	-	+	+	-
T62	Pale C, very small, flat, round, shiny, smooth	48 h	+	-	+	-	-
T63	C with clear edge, shiny, smooth, slightly raised	48 h	-	-	-	-	+
T64	Pale C, small, round, shiny, flat, smooth	48 h	+	+	+	+	+
T65	C, small, round, shiny, convex, smooth	36 h	+	+	+	+	+
T66	C, filamentous, spreading, flat	16 h	-	-	-	-	-
T67	C, small, round, shiny, raised, smooth	48 h	+	+	+	+	+
T68	C, small, round, shiny, convex, smooth	36 h	+	+	+	+	+
T69	C, round, scalloped margin, convex	16 h	-	-	+[w]	-	-
T70	C, concentric, round, shiny, crateriform, smooth	24 h	-	+[w]	+	-	-
T71	C, small, round, shiny, convex, smooth	36 h	+	+	+	+	+
T72	Pale C, umbonate, matte, rough top, smooth edge	48 h	-	-	-	-	-
T73	C, small, round, shiny, convex, smooth	36 h	-	-	+	+	-
T74	Clear C, small, round, shiny, convex, smooth	36 h	+	-	-	-	-
T75	W, very small, round, shiny, smooth	nd	-	-	-	-	-
T76	C, shiny, drop-like, smooth, round, small	36 h	-	-	-	-	+
T77	Y-C, round with ripple, clear edge, flat	24 h	+	+[w]	+	+[w]	+[w]
T78	C, concentric, round, shiny, crateriform, smooth	24 h	-	+[w]	+	-	-
T79	C, small, round, shiny, flat, smooth	16 h	-	-	-	-	-
T80	C, round, scalloped margin, convex	16 h	-	-	+[w]	-	-
T81	C, slightly scalloped, wooly, raised,	16 h	-	-	-	-	-
T82	C, round, scalloped margin, convex	16 h	-	-	-	-	-
T83	C, shiny, slightly wavy edge, slightly raised	48 h	+	+	+	+	+
T84	Y-C, very small, round, smooth, shiny, drop-like	24 h	-	-	+	+	-
T85[∞]	Y, small, round, shiny, convex, smooth	48 h	+	+	+	+[w]	+[w]
T86	Pale Y, round, smooth, matte, raised, small	48 h	+	+	+	-	+
T87	C, flat, shiny, round	36 h	-	-	-	-	-
T88	Pale C, small, round, shiny, raised, smooth	36 h	+	+	+	+[w]	-
T89	C, round, scalloped margin, convex	16 h	-	+	+	-	-
T90	C, round, scalloped margin, convex	16 h	-	-	+	-	-
T91	Clear C, small, round, shiny, convex, smooth	36 h	-	-	-	-	-
T92	Clear C, small, round, shiny, convex, smooth	5 d	+	-	+	-	-
T93	Y, small, round, shiny, convex, smooth	48 h	-	-	-	-	-
T94	Y, small, round, shiny, convex, smooth	16 h	-	-	-	-	+
T95	Pale C, round, smooth, raised margin, small, shiny	48 h	+	+	+	-	-
T96	Pale C, round, rough edges, flat, small	36 h	+	+	+	+	-
T97	Pale C, round, rough edges, flat, small	36 h	+	+	+	-	-
T98[∞]	Y, shiny, round, smooth, convex	48 h	-	+	-	+	+
T99	Pale C, wavy edge and top, slightly concave	24 h	-	-	+	+[w]	+[w]

T100	C, small shiny, smooth, flat, round, (Y in streak)	36 h	-	-	+	-	+
T101	C, small, round, shiny, convex, smooth	36 h	+	-	+	-	-
T102	Pale C, small, round, shiny, rough edges	36 h	-	+	+	+	+
T103	Pale C, small, round, shiny, wavy edges	36 h	+	+	+	+	+
T104	Pale C, small, round, shiny, wavy edges	36 h	+	+	+	+	+
T105	C, round, scalloped margin, convex	16 h	-	-	-	-	-
T106	C, round, scalloped margin, convex, shiny	16 h	-	-	-	-	-
T107	C, round, scalloped margin, convex	16 h	-	-	+	-	+
T108	Y-C, round with ripple, clear edge, flat	24 h	-	+[w]	+	+[w]	+[w]
T109	C, round, scalloped margin, convex	16 h	+	+	+	-	+
T110	C, round, rough, convex	16 h	-	+	+	-	-
T111	C, large, shiny, globular, mucoid	36 h	+	+	+	+	+
T112	C with clear margin, round, convex	16 h	-	+[w]	+[w]	-	+
T113	Pale C, small, rough edge	36 h	-	-	+	-	-
T114	C, small, shiny, slightly wavy edge, flat	nd	-	-	-	-	-
T115	C, spreading lawn, irregular edge	nd	-	-	-	-	-
T116	C, round, scalloped margin, convex	16 h	-	+	+	-	+
T117	C, round, scalloped margin, convex	16 h	-	-	+	-	-
T118	C, slightly raised, wavy top, irregular edge	nd	-	-	-	-	-
T119	C, irregular edge and top, spreading	nd	-	-	-	-	-
T121	Y-C, round with ripple, clear edge, flat	24 h	-	+[w]	+	+[w]	+[w]
T122	C, tiny, smooth, round, shiny	36 h	+	+	+	-	+
T123	Pale C, shiny, round, smooth	36 h	-	-	+	+	+
T124	Pale C, round, smooth, shiny, flat	48 h	+	+	-	+	+
T125	C, irregular edge, crateriform, shiny, smooth	36 h	-	-	+	-	-
T126	C, flat, filamentous	16 h	-	-	-	-	-
T127	C, large, irregular edge and top, spreading, raised	16 h	-	-	+	-	-
T128	C, large, irregular edge and top, spreading, raised	16 h	-	-	+	-	-
T129	C with clear margin, round, convex	16 h	-	-	-	-	-
T130	C, large, concentric, shiny, mucoid, round, convex	36 h	-	-	+	-	-
T131	C, small, shiny, crateriform, smooth, irregular edge	36 h	-	-	+	-	-
T132	Pale C, wavy edge and top, slightly concave	24 h	-	+[w]	+	-	+[w]
T133	C, small, shiny, crateriform, smooth, irregular edge	36 h	+	+	+	+	+
T134	C, very small, round, smooth, shiny, convex	48 h	+	-	+	-	+
T135	C, small, shiny, crateriform, smooth, irregular edge	36 h	+	-	+	+	+
T136	Pale C, rough edge and top, slightly concave	24 h	-	-	-	-	-
T137	Clear C, shiny, round, raised	36 h	-	-	-	+	-
T138	C, small, shiny, crateriform, smooth, irregular edge	36 h	+	-	+	-	-
T139	C, concentric, slightly wavy edge, slightly concave	24 h	+	+	+	+	+
T140	Pale Y, very small, round, smooth, shiny, convex	5 d	+	-	+	-	-
T141	Pale O, small, round, smooth, shiny, convex	9 d	-	-	+[w]	-	+
T142	C, very small, round, smooth, convex	9 d	-	-	-	-	-
T143	Pale C, wavy edge and top, slightly concave	24 h	+	+	+	+	-
T144	C, small, round, scalloped margin, convex	16 h	-	+	+	-	+
T145	C, small, round, scalloped margin, convex, shiny	16 h	-	-	+	-	+
T146	Pale C, small, round, smooth, concave	16 h	-	+[w]	+	-	+
T147[∞]	Bright Y, small, round, shiny, smooth, convex	48 h	-	-	-	-	-
T148	C-B, small, round, matte, smooth, convex	48 h	-	-	-	-	-
T149	C, small, round, scalloped margin, convex	16 h	-	-	-	-	-
T150	Dark C, round, rough edge and top, shiny, raised	48 h	-	+	+	-	-
T151	Pale C, very small, round, shiny, smooth, convex	48 h	+	+	+	-	-

T152	Pale C, very small, round, shiny, smooth, convex	nd	+	-	+	+	-
T153	C, shiny, smooth, round, raised	16 h	-	-	-	-	-
T154	C, filamentous, flat, spreading	16 h	-	-	-	-	-
T155	Pale C, concentric, flat, shiny, smooth	36 h	+	+	+	+	+
T156	C, umbonate, round, shiny	16 h	-	-	-	-	-
T157	C, filamentous, flat, spreading	16 h	-	-	-	-	-
T158	Pale Y, powdery W top, small, round, convex	36 h	-	-	-	-	-
T159	C, round, scalloped margin, convex, shiny	16 h	-	-	-	-	-
T160	C, shiny, round, smooth, slightly raised	36 h	-	-	+	-	+
T161	C, shiny, irregular top, fibrous edges, crateriform	36 h	-	+	+	-	+
T162	Clear C, small, round, shiny, convex, smooth	5 d	+	-	+	-	-
T163	Dark C, large, shiny, irregular edge and top	36 h	-	-	-	-	-
T164	C, scalloped edge, convex, rough top	48 h	-	-	-	-	-
T165	O-K, small, shiny, round, smooth, convex	nd	-	-	-	-	-
T166	Pale C, raised edge, wooly, slightly concave	24 h	+	+	+	+	-
T167	C with clear margin, round, convex	16 h	-	+	+	-	+[w]
T168	Cream, concentric, round, smooth, raised	36 h	+	+	+	+	-
T169	Pale C, round, concentric, smooth, raised edge	36 h	-	+	+	+	+
T170	W, very small, round, smooth, shiny	nd	-	-	-	-	-
T171	Clear C, very small, shiny, smooth, raised	16 h	-	-	-	-	-
T172	C, wavy edge, convex, shiny	24 h	+	+	+	+	+
T173	C edge, W middle, round, smooth, slightly raised	36 h	+	+	+	-	+
T174	Dark C, large, irregular top, round, wavy edge	36 h	-	-	-	-	-
T175	C, wavy edge, convex, shiny	24 h	+	+	+	+	+
T176	O, small, round, smooth, convex, hard	nd	-	-	-	-	-
T177	Dark O, smooth, round, shiny, convex	36 h	-	-	-	-	-
T178	Pale C, round, flat, smooth, shiny	36 h	+	+	+	+	+
T179	C, extremely mucoid	5 d	-	+	+	-	+
T180	C, raised, shiny, round, smooth	36 h	+	+	+	+	+
T181	Pale Y, shiny, round, raised	36 h	-	+[w]	+	+	+
T182	C, small, round, smooth, shiny, raised	24 h	-	-	-	-	-
T183	C, shiny, raised edge, round, slightly rough	48 h	+	+	+	+	+
T184	C, very opaque, smooth, round, shiny, drop-like	nd	-	+	+	-	-
T185	C, very opaque, smooth, round, shiny, drop-like	48 h	-	+	+	-	-
T186	C, very small, round smooth, convex, shiny	nd	-	-	-	-	-
T187[∞]	Y, small, round, smooth, shiny, convex	5 d	-	+	-	-	+[w]
T188	C, round, smooth, flat, shiny	48 h	-	-	-	-	-
T189	Pale C, wrinkled, round, shiny	36 h	+	+	+	+	+
T190	C, irregular edge, powdery top	5 d	-	-	-	-	-
T191	C, round, scalloped margin, convex, shiny	16 h	-	-	-	-	-
T192	Dark C, mucoid, shiny, round, smooth	36 h	-	-	+	-	-
T193	Dark C, round, slightly raised	16 h	-	-	-	-	-
T194	C, small, round, matte, convex	nd	-	-	+	+	-
T195	C, raised edge, wooly, slightly concave	nd	-	-	+	-	+
T196	C, shiny, round, smooth, convex	16 h	-	+	+	-	-
T197	Dark C, large, round, irregular edge, shiny, raised	36 h	+	-	+	+	+
T198	C, round, small, shiny, smooth	nd	-	-	-	-	-
T199	Dark C, shiny, irregular edge, raised	16 h	-	-	-	-	-
T200	Dark C, large, round, scalloped edge, flat, shiny	36 h	-	-	-	-	-
T201	Dark Y-C, irregular top, round, matte	36 h	-	-	-	-	-
T202[∞]	Bright Y, small, shiny, round, smooth, convex	36 h	+	+	+	-	+[w]

T203	C, smooth, round, shiny, raised	36 h	-	-	-	-	-
T204	C, round, scalloped margin, convex	16 h	-	-	-	-	-
T205[∞]	Y, small, round, shiny, smooth, convex	48 h	-	-	-	+	-
T206	Pale C, shiny, scalloped and raised edge, round	36 h	+	+	+	+	+
T207	Dark C, large, round, scalloped edge, flat, rough	48h	-	-	-	-	-
T208	Dark C, round, smooth, flat	36 h	-	-	-	-	-
T209	W, very small, round, shiny, smooth	nd	-	-	-	-	-
T210	Pale C, irregular edge, smooth, shiny, flat	48 h	-	-	+	-	-
T211	C, round, scalloped edge, flat, shiny	36 h	-	-	-	-	+
T212	Clear, small, very shiny, round, smooth, convex	5 d	+	-	+	+	+
T213	Pale C, small, shiny, round, smooth	36 h	-	-	+	-	+
T214	C, irregular edge, rough top, slightly raised	36 h	-	+	+	-	+
T215	C, Very small, shiny, smooth, round, convex	16 h	-	-	-	-	-
T216	C, shiny middle, powdery edge, flat	36 h	+	+	+	-	-
T217	C, shiny middle, powdery edge, flat	36 h	+	+	+	-	-
T218	Clear, very small, round, shiny, smooth	nd	-	-	-	-	-
T219	Pale C, W in middle, irregular edge	36 h	+	+	+	+	+

***** B, brown; C, cream; K, pink; O, orange; P, purple; R, red; W, white; Y, yellow

† Time when colonies were first visible after plating from gut extracts; h, hours; d, days

‡ MUA, MUC, MUG, MUM, and MUX are 4-methylumbelliferyl-α-L-arabinofuranoside, 4-methylumbelliferyl-β-D-cellobioside, 4-methylumbelliferyl-β-D-glucopyranoside, 4-methylumbelliferyl-β-D-mannopyranoside, and 4-methylumbelliferyl-β-D-xylopyranoside, respectively.

\+ Positive result

\+ [w] Weak positive result

\- Negative Result

∞ Isolates with similar morphology to previous isolate C3.

§ nd, not determined

The ten isolates (T34, T35, T39, T41, T85, T98, T147, T187, T202, and T205) with similar morphology to the bacterium C3, previously isolated from the *T. abdominalis* gut, were bright yellow, round, smooth, shiny, convex, and small (Table 2.1). Analysis of 16S rRNA partial sequences (~500 bp) revealed that four of the isolates (T34, T 35, T39, and T41) were 100 % identical to each other and had 95 % identity to a *Caulobacteraceae* sp. (Table 2.2). However, only two of these four isolates (T31 and T39) displayed similar activities on plates containing MU-conjugated sugars. Two of the ten isolates (T85 and T205) had 96 % sequence identity to *Agromyces albus*, but were not 100 % identical to each other. One isolate (T147) had 100 % sequence identity to *Cellulomonas turbata* and another (T98) had 98 % sequence identity

to an unidentified *Cellulomonas* sp. Another of the ten isolates (T187) had 97 % sequence identity to *Sanguibacter suarezii*, and the last isolate (T202) had 95 % identity to *Agrococcus jenensis* (Table 2.2).

Table 2.2. Isolate identification via partial16S rRNA sequence and screening results on media containing MU-conjugated sugars.

Isolate	Closest Match	**Accession Number**	**Percent Identity**	**MUA**	**MUC**	**MUG**	**MUM**	**MUX**
T 34	*Caulobacteraceae sp.*	AY504429	95	+	-	-	-	-
T 35	*Caulobacteraceae sp.*	AY504429	95	+	+	+	-	-
T 39	*Caulobacteraceae sp.*	AY504429	95	+	-	-	-	-
T 41	*Caulobacteraceae sp.*	AY504429	95	+	+	-	-	-
T 85	*Agromyces albus*	AF50391	96	+	+	+	$+^{w}$	$+^{w}$
T 98	*Cellulomonas sp.*	Y09658	98	-	+	+	+	+
T 147	*Cellulomonas turbata*	X79454	100	-	-	-	-	-
T 187	*Sanguibacter suarezii*	AY5044	97	-	+	+	-	$+^{w}$
T 202	*Agrococcus jenensis*	X92492	94	+	+	+	-	+
T 205	*Agromyces albus*	AF50391	96	-	-	-	$+^{w}$	-

\+ Positive reaction
$+^{w}$ Weak positive reaction
\- Negative reaction

Discussion

Cellulase and hemicellulase activity have been successfully demonstrated in hindgut extracts of *T. abdominalis* larvae by use of MU-conjugated model substrates. Since the MU-conjugated sugars resemble ends of large polymeric sugars or oligosaccharides, hindgut extracts demonstrated enzyme activity degrading sugar polymer ends or oligosaccharides produced by the partial degradation of lignocellulosic material. No cellulolytic or hemicellulolytic activity

was detected within the midgut, which is not surprising because the pH of the midgut suggests proteolytic, not cellulolytic or hemicellulolytic activity.

Enzyme activity profiles were similar for animals in captivity for 14, 23, and 28 days, therefore demonstrating that captivity between days 14 and 28 had a minimal affect on the detection of hydrolytic enzyme capabilities. Larvae were not assayed on the day of capture; therefore it cannot be determined if a change in hydrolytic enzyme activity occurred between days 0 and 14. It is probable that as food sources change, a shift will occur in the microbial community and/or enzyme production to allow for better degradation of the new food source. In this study, larvae were fed leaves collected from the stream of capture to reduce a potential shift in the microbial community or enzyme production.

Fermentation of the cellulolytic larval diet is expected within the hindgut since it possesses an enlarged anterior paunch, which is an analogous structure to the termite paunch where fermentation is facilitated by retarding the passage of food through the hindgut (Klug & Kotarski 1980, Martin 1987b) (Figure 2.5). Also, both the degradation of cellulose to organic acids and the transport of acetate into the hemolymph as a carbon and energy source for *T. abdominalis* have been demonstrated (Lawson et al 1984, Sinsabaugh et al 1985b). Future studies will include enzyme activity analysis of the anterior paunch verses the posterior hindgut to determine where the majority of the cellulose degradation occurrs.

Isolation of gut-associated bacteria was performed under aerobic conditions on rich media (TSA and LBA). No special efforts were made to enrich for cellulolytic or hemicellulolytic bacteria or to isolate anaerobes because the culturing techniques were originally designed for comparing the quantity of bacteria in the enzyme extracts and resuspended gut extracts to the boiled and filtered controls. It was only after isolation that the magnitude of

morphological diversity that can be found by using readily available media was realized. Other studies from this research group have cultured bacteria from various areas of the *T. abdominalis* alimentary tract with various types of media under both aerobic and anaerobic conditions (Peterson, unpublished data).

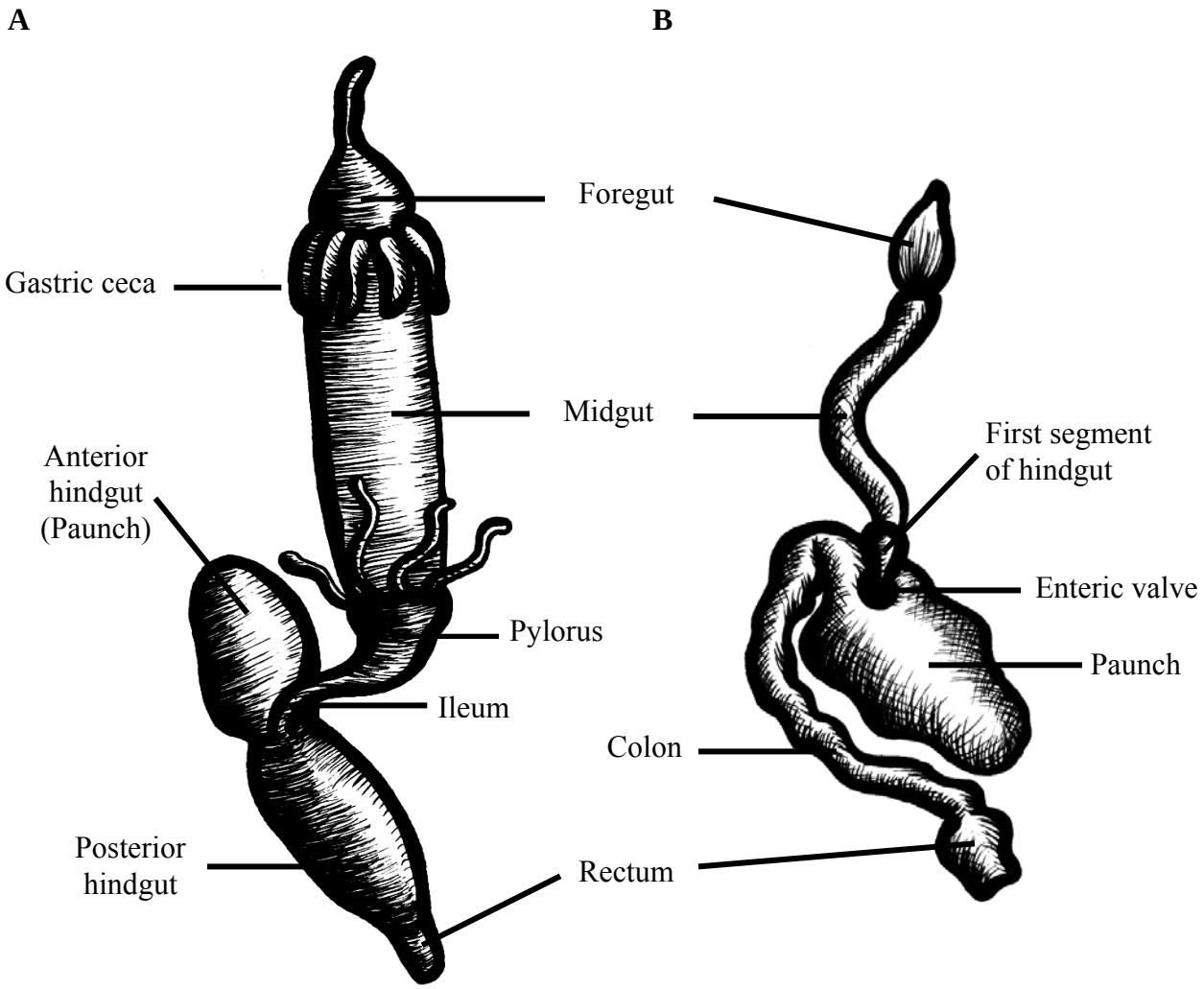

Figure 2.5. Crane fly (*T. abdominalis*) and termite (*Macrotermes natalensis*) alimentary systems. A. *T. abdominalis* alimentary tract is redrawn from Klug and Kotarski, 1980. B. *M. natalensis* alimentary tract is redrawn from Martin, 1987. Figures are not drawn to scale.

CHAPTER 3

CROCEBACTERIUM ILECOLA GEN. NOV., SP. NOV. ISOLATED FROM THE HINDGUT OF A *TIPULA ABDOMINALIS* LARVA[1]

[1] Rogers, T.E. and J.B. Peterson. To be submitted to IJSEM.

Abstract

A member of the family *Microbacteriaceae* was isolated from the hindgut of the aquatic crane fly, *Tipula abdominalis*. Taxonomic position of the isolate within this family was determined by a polyphasic approach, as is commonly employed for the separation of genera within the family *Microbacteriaceae*. The bacterial isolate is Gram-type positive, motile, nonsporulating, and rod-shaped. The G + C content of the DNA is 64.9 mol %. The cell wall contains B2γ type peptidoglycan, D- and L-diaminobutyric acid as the diamino acid, and rhamnose as the predominant sugar. The predominant fatty acids are 12-methyltetradecanoic acid (ai-$C_{15:0}$) and 14-methylhexadecanoic acid (ai-$C_{17:0}$). The isolate forms a distinct lineage within the family *Microbacteriaceae*, as determined by 16S rRNA sequence analysis. We propose the name *Crocebacterium ilecola* gen, nov., sp. nov., to accommodate this bacterial isolate. The type species is $T202^T$.

Introduction

Larvae of the aquatic crane fly *Tipula abdominalis* (Say) (Diptera: Tipulidae) are major shredders of leaf detritus in heterotrophic stream ecosystems worldwide (Lawson et al 1984, Martin 1987b, Petersen et al 1989, Sinsabaugh et al 1985b). Like many other insects, *T. abdominalis* larvae have microbial symbionts residing in the alimentary tract (Dillon & Dillon 2004). This microbial community was studied via microscopy and direct isolation, revealing great morphological diversity on the posterior hindgut wall (Klug & Kotarski 1980). Current genetic and isolation studies are uncovering many novel genera and species from the *T. abdominalis* gut system (Peterson, unpublished data). This paper describes the isolation of strain $T202^T$ from the hindgut of a *T. abdominalis* larva. Characterization was performed using a polyphasic approach, which differentiates taxonomic lineages by assessing both phylogenetic

and phenotypic characteristics. Based on the phylogenetic and chemotaxonomic data presented within, we propose a novel genus within the family *Microbacteriaceae*, *Crocebacterium* gen. nov., and the type species, *Crocebacterium ilecola* sp. nov., to accommodate this bacterium.

Methods

Collection and Dissection of Larvae

Fourth instar *T. abdominalis* larvae were collected from Shope Fork Creek at the Coweeta Hydrological Laboratory, N.C. during the month of March 2004. Stream parameters were as follows: pH 5.35; dissolved oxygen, 11.2 mg l^{-1}; water temperature, 7.7 ˚C; conductivity, 14.58 µs cm^{-1}; turbidity, 0.47 NTU; alkalinity, 12.0 mg l^{-1}; <1 mg NO_3^- l^{-1}; and <0.1 mg PO_4^{3-} l^{-1}. Larvae were stored at 12 ºC in an aerated 4 L container filled with filter-sterilized stream water and leaves collected from the stream of capture. Water was exchanged with fresh stream water every three to four days until dissection three weeks after capture. *T. abdominalis* larval guts were removed during dissection under buffering salt solution (BSS), pH 7.4 (Leadbetter & Breznak 1996). Hindguts were separated from the rest of the alimentary system and placed in 5 ml BSS, pH 7.4. Hindguts were sonicated in a Branson 1510 ultrasonic bath for 1 min to displace bacteria attached to the gut wall and then centrifuged at 3,500 x g at 4 ˚C for 30 min (Schulte et al 2003). The supernatant and pellet were separated, and the pellet was resuspended in 5 ml BSS, pH 7.4.

Bacterial Isolation and Maintenance

Aliquots of the gut homogenate supernatant and resuspended pellet (50 µl) were plated onto tryptic soy agar (TSA, DIFCO) and Luria-Bertani agar (LBA, DIFCO) and incubated at room temperature until colonies appeared. Colonies were streaked on TSA or LBA for isolation, and then glycerol stocks (40 % v/v) were made and stored at – 80 °C.

Morphological and Physiological Characteristics

Isolate T202^T colony morphology was studied on TSA at 24 – 25 °C. Cell morphology was studied by phase-contrast microscopy and bright-field microscopy. Gram-staining was performed as described (Ayers 2000). Motility was studied by phase-contrast microscopy and motility test medium (BBL) (2003b). Temperature range and optimum for growth were determined in TSB, pH 7.0. For temperatures above 5 °C, a temperature gradient incubator (Scientific Industries, Bohemia, N.Y.) was used with agitation. For temperatures between 0 and 5 °C, cells were grown on TSA, pH 7.0. pH range and optimum for growth were determined in TSB at 24 – 25 °C. NaCl tolerance was determined on LBA with NaCl concentrations between 0 and 10 % (w/v). Growth under anaerobic and microaerobic conditions was examined using BBL GasPak® jar systems. Presence of endospores was determined by staining as previously described (Doetsch 1981).

Isolate T202^T was grown at 24 – 25 °C for all physiological tests mentioned below. Catalase activity was determined by the addition of 3 % (v/v) hydrogen peroxide solution. Oxidase activity was tested using freshly prepared 1 % tetramethyl-*p*-phenylenediamine dihydrochloride (Tarrand & Groschel 1982). Methyl red (MR), Voges-Proskauer (VP), nitrate reduction, formation of H_2S, urease activity, extracellular DNase activity, and hydrolysis of

casein and starch were determined following the manufacturer's instructions (DIFCO) (2003b). Hydrolysis of carboxymethyl cellulose (CMC), xylan, and pectin was determined as previously described (2003b, MacFaddin 1985, Mondou et al 1986, Vera & Dumoff 1974, Wood & Kellogg 1988). Various enzyme activities and acid production from a variety of carbohydrates were investigated using API Staph, Strep, and Coryne systems (bioMérieux) following the manufacturer's instructions, except incubation was at 25 ˚C for 48 hours. Cleavage of methylumbelliferyl (MU) conjugated sugars, 4-methylumbelliferyl-α-L-arabinofuranoside (MUA, Sigma), 4-methylumbelliferyl-β-D-cellobioside (MUC, Sigma), 4-methylumbelliferyl-β-D-glucopyranoside (MUG, Sigma), 4-methylumbelliferyl-β-D-mannopyranoside (MUM, Sigma), and 4-methylumbelliferyl-β-D-xylopyranoside (MUX, Sigma) was determined by the method of Sharrok, 1988. Antibiotic tolerance was determined by the Kirby-Bauer disc-diffusion method using BBL^{TM} Sensi-Discs (2003a).

Chemotaxonomic Characteristics

Cell wall analysis was performed by the DSMZ identification service (Braunschweig, Germany). Peptidoglycan structure was analyzed as described by (Schleifer & Kandler 1972) and (Schleifer 1985). Amino acid quantification was performed by gas chromatography (MacKenzie 1987). Sugars present in the cell wall were determined as described by (Staneck & Roberts 1974). Fatty acid methylesterase (FAME) analysis was performed by MIDI LABS (Newark, DE).

DNA Extraction and Phylogenetic Analysis

DNA extraction was modified from Harwood and Cutting, 1990. Briefly, pelleted cells were resuspended in lysis buffer (50 mM Na_2EDTA, 0.1 M NaCl, pH 7.5) with 3 mg lysozyme ml^{-1} and incubated at 37 °C for 10 min. SDS was added to 1.5 % (w/v) final concentration, and the sample was incubated an additional 5 min at 37 °C. Phenol (pH 7.8) extraction, chloroform:isoamyl alcohol (24:1) extraction, and ethanol precipitation were then performed. DNA G + C content was determined as described in Mesbah *et al*. (1989) and confirmed by the DSMZ by the methods of (Cashion et al 1977, Mesbah & Whitman 1989, Tamaoka & Komagata 1984, Visuvanathan et al 1989). Sequencing of the full 16S rRNA gene was performed by MIDI LABS using primers corresponding to *Escherichia coli* 16S rRNA positions 005 and 1540. Sequences with high similarity to isolate $T202^T$ were obtained from a BLAST search with GenBank (http://www.ncbi.nlm.nih.gov). The 16S rRNA gene sequence from isolate $T202^T$ was aligned with the multiple alignment program ClustalX (Thompson et al 1997) against previously determined *Microbacteriaceae* sequences obtained from the public database NCBI (http://www.ncbi.nlm.nih.gov), then edited with GeneDoc (Nicholas et al 1997). Phylogenetic analyses were performed with the program Mega2 (Mukhopadhyay et al 2005). To determine consistency between analysis methods, phlyogenetic distance trees were generated using the Kimura two-parameter and Jukes-Cantor models and the neighbor-joining, minimum evolution, and maximum parsimony algorithms (Kimura 1980, Saitou & Imanishi 1989).

Results and Discussion

Morphological and Physiological Characteristics

Isolate T202^T colonies were round, smooth, shiny, convex, opaque, yellow when grown in the light, and white when grown in the dark. Long rods were the predominant morphology in young cultures (width 0.7 – 1.5 μm, length 3 – 4.5 μm, ~18 hrs), and short rods predominate older cultures (width 0.4 – 0.7 μm, length 0.7 – 1.5 μm, ~50 hrs), yet a marked rod-coccus cycle was not observed. When cells were longer, they often occurred in short chains of two to four cells, each at a slight angle to the other at the point of attachment. Gram stain was negative for a young culture (~18 hrs), and positive for an older culture (~50 hrs). Motility was greater in younger cultures than older cultures (~18 hrs and ~50 hrs, respectively). Optimal cell growth was at 21-25 °C, pH 7.0, and 0.0 - 0.5 % (w/v) NaCl. Weak growth occurred at 0 and 37 °C, pH 10, and 2.5 % (w/v) NaCl. No growth occurred at 42 °C, pH 5, and 5 % (w/v) NaCl. Cells grew best aerobically, and less growth occurred under microaerobic conditions. Growth was not detected after a four-week incubation under anaerobic conditions, but growth occurred when transferred to aerobic conditions. Cells did not form endospores. A long to short rod cycle, variable Gram stain, lack of sporulation, microaerobic growth, and minimum growth temperatures near 0 °C are characteristics found among many members of the *Microbacteriaceae* family (Groth et al 1996, Kampfer et al 2000, Mannisto et al 2000, Sheridan et al 2003, Zlamala et al 2002).

Catalase and oxidase tests were positive. Nitrate was reduced to NH_4^+. MR and VP tests were negative, and isolate T202^T did not form H_2S. No hydrolysis of hippurate, gelatin, casein, starch, CMC, xylan, or pectin occurred. Isolate T202^T tested positive for the enzyme activities of alkaline phosphatase, β-glucosidase, α-glucosidase, β-glucuronidase, β-galactosidase, and urease.

T202^T did not produce α-methyl-D-glucosidase, N-acetyl-glucosaminase, α-galactosidase, leucine arylamidase, citrase, or pyrrolidonyl arylamidase. Under aerobic conditions, acid was produced from D-glucose, D-fructose, D-mannose, D-maltose, lactose, D-trehalose, D-mannitol, xylitol, D-melibiose, raffinose, xylose, and sucrose. Since growth did not occur under anaerobic conditions, acid production from carbohydrates under anaerobic conditions was not detected. Degradation of MUA, MUC, MUG, and MUX occurred. MUM was not degraded. Isolate T202^T was resistant to kanamycin (30 μg) and penicillin (10 μg), but not to ampicillin (10 μg), ciprofloxacin (5 μg), erythromycin (15 μg), rifampin (5 μg), polymyxin B (300 μg), streptomycin (10 μg), trimethoprim (5 μg), or vancomycin (30 μg).

Chemotaxonomic Characteristics

The cell wall peptidoglycan was of the type B2γ. The cell wall contained alanine, glycine, D- and L-diaminobutyric acid (DAB), and glutamic acid in the molar ratio 0.6 : 1.0 : 2.5 : 1.0. The predominant sugar in the cell wall was rhamnose, and the minor sugar was mannose. No mycolic acids were present. The most abundant lipids were 12-methyltetradecanoic acid (ai-$C_{15:0}$; 63.5 %) and 14-methylhexadecanoic acid (ai-$C_{17:0}$; 21.0 %). Other lipids present in significant amounts were 13-methyltetradecanoic acid (i-$C_{15:0}$; 1.35 %), hexadecanoic acid ($C_{16:0}$; 5.09 %) and 14-methylpentadecanoic acid (i-$C_{16:0}$; 7.03 %). Tetradecanoic acid ($C_{14:0}$), 12-methyltridecanoic acid (i-$C_{14:0}$), pentadecanoic acid ($C_{15:0}$), 15-methylhexadecanoic acid (i-$C_{17:0}$), octadecanoic acid ($C_{18:0}$), and cyclohexyl acid w9c-18:1 were each present as less than one percent.

DNA Extraction and Phylogenetic Analysis

The G + C content of the DNA was 64.9 mol %. Isolate T202^T full rRNA gene sequence (1,526 nucleotides) had 96.5 % identity to an unidentified actinobacterium (partial sequence) cultured from African millipede fecal pellets. Both an uncultured actinobacterium from an industrial biofilter (partial sequence) (Friedrich et al 2002) and a *Leifsonia poae* isolate from nematode galls (partial sequence) (Evtushenko et al 2000) had 96.2 % sequence identity to isolate T202^T 16S rDNA.

Taxonomic Conclusions

Results from phylogenetic distance analyses were similar using the Kimura two-parameter or Jukes-Cantor model and the neighbor-joining, minimun evolution, or maximum parsimony algorithm. Phylogenetic trees based on these distance analyses show that isolate T202^T is closely related to the genera *Agreia, Frigoribacter, Subtercola*, *Rhodoglobus,* and *Salinibacterium,* yet forms a distinct lineage among these genera within the *Microbacteriaceae* family (Figure 3.1). Isolate T202^T is shown to cluster with the genus *Frigoribacterium*, but the bootstrap value is low (39) indicating that this placement is uncertain. Other characteristics separating isolate T202^T from other genera within this cluster are the cell wall amino and diamino acids, cell wall sugars, fatty acid profile, and menaquinone composition (Table 3.1). Most notably different are the fatty acids with ai-$C_{15:0}$ composing over 60 % of the total fatty acids. The genus *Rhodoglobus* has the closest fatty acid composition with 53.2 % ai-$C_{15:0}$ and 22.6 % ai-$C_{17:0}$, but this genus has 18.8 % i-$C_{16:0}$ compared to 7.0 % for isolate T202^T. Also, the genus *Rhodoglobus* has D-ornithine as the diamino acid within the cell wall, whereas isolate T202^T has D- and L-DAB (Table 3.1).

Although isolate T202^T has up to 96.2 % sequence identity to other genera within the family *Microbacteriaceae*, this high percent identity is common between members of other genera within this family. For example, the 16S rRNA sequence identities of the genera *Agreia* and *Subtercola* are 96.8 – 97.1 %, and identities for *Frigoribacterium*, *Rathayibacter,* and *Clavibacter* are 96.1 – 97.1 % (Evtushenko et al 2001, Kampfer et al 2000). These were characterized as separate genera based on polyphasic taxonomic studies rather than 16S rRNA sequence similarity alone. Of the phenotypic properties studied, chemotaxanomic characteristics, such as peptidoglycan composition, and fatty acid profile, were important distinguishing characteristics between these genera (Evtushenko et al 2002, Tsukamoto et al 2001). Considering both chemotaxanomic characteristics and 16S rRNA analysis, isolate T202^T clearly forms a separate genus within the family *Microbacteriaceae*. We propose a new genus within the *Microbacteriaceae* family, *Crocebacterium* gen. nov., and the type species, *Crocebacterium ilecola* sp. nov., to accommodate this bacterial isolate.

Ecology

Many members of the *Microbacteriaceae* family are associated with plants (Behrendt et al 2002, Dorofeeva et al 2002, Dorofeeva et al 2003, Evtushenko et al 2001, Evtushenko et al 2002, Evtushenko et al 2000, Sasaki et al 1998). The source of inoculum for the *T. abdominalis* hindgut is believed to be ingested leaf detritus (Klug & Kotarski 1980, Lawson et al 1984); therefore it is not surprising to find members of the *Microbacteriaceae* family within this gut system. Additionally, this bacterium was most likely a gut wall-associated bacterium since it was isolated from the pelleted hindgut (Dillon & Dillon 2004). Most gut wall-associated bacteria are considered resident rather than transient bacteria, because they can resist the flow of

material through the gut by attachment or inhabiting small crevices along the gut wall (Harris, 1992)(Dillon & Dillon 2004). Because these bacteria are constant inhabitants of the hindgut, they may have a specific role within the microbial community. One possible role is the degradation of cellulosic material in the *T. abdominalis* larval gut (Dillon & Dillon 2004, Sinsabaugh et al 1985b). Although isolate T202^T was unable to hydrolyze large polymeric carbohydrates such as starch, CMC, and xylan, it was able to cleave four of the five MU-conjugated sugars tested. If isolate T202^T is a resident of the hindgut, it may occupy a niche within the microbial community degrading oligosaccharides produced by the partial degradation of lignocellulosic material. To determine whether this bacterial isolate, or any other isolate from the *T. abdominalis* hindgut, is a resident rather than a transient bacterium, studies such as fluorescent in situ hybridization may be employed.

Description of *Crocebacterium* gen. nov.

Crocebacterium (Cro.ce.bac.ter.ium. L. adj. *croceus* saffron-colored, golden, yellow; Gr. n. *bakterion* small rod; *Crocebacterium* a small yellow bacterium).

Cells are microaerobic to aerobic, Gram-type positive, high-G + C, motile, non-spore-forming, irregular rods. Colonies are round, smooth, shiny, convex, opaque, and may produce pigments. Growth occurs at mesophilic temperatures and neutral pH. The cell wall peptidoglycan is of the type B2γ, and the diamino acid is D- and L-DAB. No mycolic acids are present. Predominant fatty acids are 12-methyltetradecanoic acid (ai-$C_{15:0}$) and 14-methylhexadecanoic acid (ai-$C_{17:0}$). The type species is *Crocebacterium ilecola*^{T}.

Description of *Crocebacterium ilecola* sp. nov.

Crocebacterium ilecola (i.le.co.la. L. n. *ile* gut; Gr. adj. *–cola* inhabitant; *ilecola* inhabitant of the gut).

In addition to those characteristics described for the genus, *Crocebacterium ilecola* does not have a marked rod – coccus cycle. Cells of younger cultures are motile, long rods, and stain Gram-negative, and cells of older cultures are less motile, shorter rods, and stain Gram-positive. Colonies are yellow when grown in the light, and white when grown in the dark. The DNA G + C content is approximately 65 mol %. Cell wall amino acids are alanine, glycine, D- and L-DAB, and glutamic acid (0.6 : 1.0 : 2.5 : 1.0 molar ratio). Cell wall sugars are rhamnose (major) and mannose (Rondon et al). Temperature range for growth is 0 – 37 °C, optimal growth occurs between 21 – 25 °C, and no growth occurs at occurs at 42 °C. Growth occurs at a pH range of 6 – 10, optimal growth occurs at and pH 7.0, and no growth occurs at pH 5.0. Range of NaCl concentrations for growth is 0 – 2.5 % (w/v), optimal growth occurs between 0.0 – 0.5 % (w/v) NaCl, and growth is inhibited at 5.0 % (w/v) NaCl. Catalase and oxidase positive. Nitrate was reduced to NH_4^+. MR and VP tests were negative. Activities were positive for alkaline phosphatase, β-glucosidase, α-glucosidase, β-glucuronidase, β-galactosidase, and urease. Under aerobic conditions, acid is formed from D-glucose, D-fructose, D-mannose, D-maltose, lactose, D-trehalose, D-mannitol, xylitol, D-melibiose, raffinose, xylose, or sucrose. Hippurate, gelatin, casein, starch, CMC, xylan, and pectin are not hydrolyzed. Resistant to kanamycin (30 μg) and penicillin (10 μg), but susceptible to ampicillin (10 μg), ciprofloxacin (5 μg), erythromycin (15 μg), rifampin (5 μg), polymyxin B (300 μg), streptomycin (10 μg), trimethoprim (5 μg), and vancomycin (30 μg).

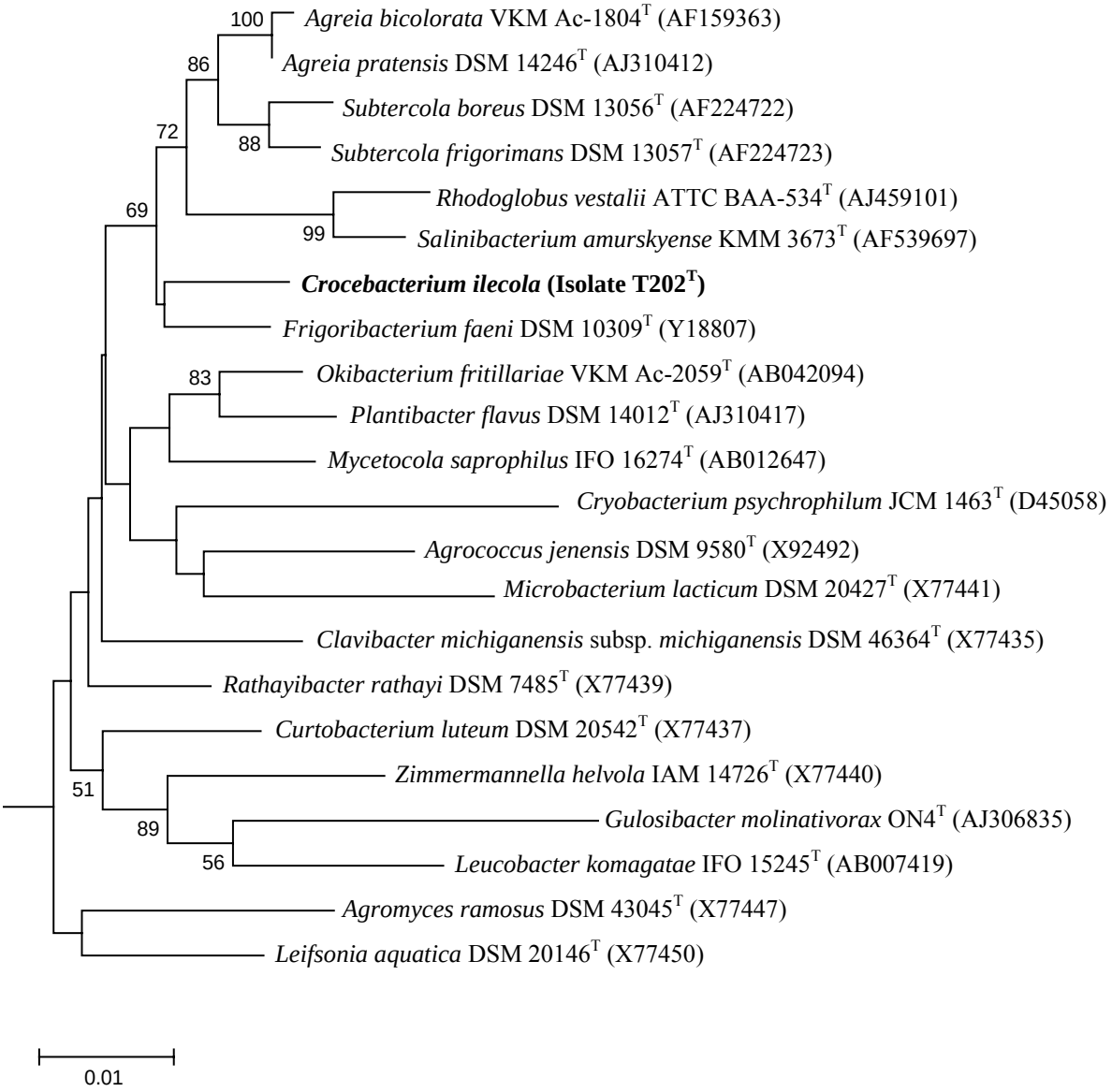

Figure 3.1. Phylogenetic tree based on 16S rRNA gene sequences of *Crocebacterium ilecola* and genera of the family *Microbacteriaceae*. Accession numbers for nucleotide sequences are in parentheses. The numbers on the tree indicate bootstrap values, expressed as a percentage of 500 replicates. Only bootstrap values of 50 % or greater are shown. Bar indicates 1 nucleotide substitution per 100 nucleotides. *Brevibacter linens* (DSM 20425^T, X77451) served as an outgroup sequence to estimate the root position of the tree.

Table 3.1. Distinguishing characteristics of the genera *Agreia, Rhodoglobus, Salinibacterium, Subtercola,* and isolate T202^T.

Data collected from (Behrendt et al 2002), (Evtushenko et al 2001), (Kyun Han et al 2003), Mannisto *et al*. (2003), (Sheridan et al 2003), (Schumann et al 2003).

Characteristic	Isolate T202^T	*Agreia*	*Frigoribacterium*	*Rhodoglobus*	*Salinibacterium*	*Subtercola*
Peptidoglycan type*	B2γ	B	B2β	B2α	B	B2γ
Cell wall diamino acids†	D, L-DAB	L-DAB, D-Orn	D-Lys	D-Orn	D-Lys, D-Orn	DAB
Other cell wall amino acids‡	Ala, Gly, Glu	Ala, Gly, Hyg or Glu	Ala, Gly, Hsr	Ala, Gly, Glu	Ala, Gly, Glu	?Hyg
Cell wall sugars - major	Rhamnose	Rhamnose	nr§	nr	nr	Rhamnose, Xylose
- minor	Mannose	Mannose and Fucose	nr	nr	nr	Mannose, Glu, Rib
Major fatty acids (%)‖						
ai-$C_{17:0}$¶	21.0	14.4 – 22.1	7.0 – 14.8	22.6	2.8	3.5 – 6.8
ai-$C_{15:0}$	63.5	46.7 – 48.0	37.8 – 48.3	53.2	40.4	46.1 – 51.6
i-$C_{16:0}$	7.0	17.2 – 30.1	10.0 – 16.7	18.8	34.7	4.2 – 10.2
i-$C_{15:0}$	1.3	≤ 1.0	1.3 – 1.8	0.79	6.6	< 1.0 – 4.3
i-$C_{14:0}$	< 1.0	< 1.0	≤ 1.0	1.1	14.7	< 1.0 – 6.7
$C_{16:0}$	5.1	2.7 – 5.2	4.4 – 26.5	0.55	-	-
Major Menaquinones	nr	10	9	11, 12	11	9, 10
G+ C content (mol %)	65	65 – 67	71.1	62	61	64 – 68
Temperature optima (°C)	21 – 25	24 – 26	4 – 8	18	25 – 28	15 – 17
Temperature range (°C)	1 – 37	< 37	-2 – 28	-2 – 21	4 – 37	-2 – 28
Motility	+	+	+	nr	-	-
Colony color#	Y, W	Y, O	Y	R	nr	Y

* Peptidoglycan type as designated by Schleifer and Kandler (1972).
† DAB, diaminobutyric acid; Lys, lysine; Orn, ornithine
‡ Ala, alanine; Gly, glycine; Glu, glutimate; Hsr, homoserine; Hyg, hydroxyglutamate.
§ Growth temperature: Isolate T202^T, 25 °C; *Agreia*, 25 °C; *Frigoribacterium*, 28 °C; *Rhodoglobus*, 18 °C; *Salinibacterium*, ; *Subtercola*, 25 °C.
‖ ai, Anteiso-branched fatty acids; i, iso-branched fatty acids
¶ nr, Not reported.
# R, Red; W, white; Y, yellow.

CHAPTER 4

CONSTRUCTION OF *CROCEBACTERIUM ILECOLA* GENOMIC LIBRARY AND SCREEN FOR CELLULASE AND HEMICELLULASE ACTIVITY

Introduction

Crocebacterium ilecola is a Gram-type positive bacterium isolated from the hindgut of the aquatic crane fly *Tipula abdominalis*, a detritus shredder abundant in small order stream ecosystems. The microbial consortium within the *T. abdominalis* hindgut is hypothesized to be responsible for degrading the lignocellulosic diet ingested by the insect (Sinsabaugh et al 1985b). *C. ilecola* is unable to hydrolyze large polymeric carbohydrates such as starch and xylan. This bacterium can, however, degrade the methylumbelliferyl- (MU) conjugated sugars 4-methylumbelliferyl-α-L-arabinofuranoside (MUA), 4-methylumbelliferyl-β-D-cellobioside (MUC), 4-methylumbelliferyl-β-D-glucopyranoside (MUG), and 4-methylumbelliferyl-β-D-xyloside (MUX). The MU-conjugated sugars resemble sugar polymer ends and oligosaccharides produced by degradation of the larger polymeric sugars. Although *C. ilecola* is unable to degrade lignocellulosic material alone, it may be occupying a niche within the *T. abdominalis* hindgut microbial community degrading sugar polymer ends and oligosaccharides.

To further study the cellulose and hemicellulose degradative abilities of *C. ilecola*, a genomic library was constructed and screened for activity on the four MU-conjugated sugars that the isolate was able to degrade. Since many bacterial cellulases and hemicellulases are encoded by gene sequences of 1 – 2 kb (NCBI-GENE, http://www.ncbi.nlm.nih.gov), the library was constructed to contain 2.5 – 5.0 kb genomic DNA. The expression vector pUC19 was chosen for

cloning since it is a high copy number plasmid and can maintain the desired DNA segment sizes (Lin-Chao et al 1992, Miki 1987, Yanisch-Perron et al 1985).

Methods

Vector Preparation

The plasmid vector pUC19 (NEB) was extracted from *Escherichia coli* DH5α (F$^-$*sup*E44 deoR*lac*U169 [Φ80 *lacZΔM15*] *hsdR17* [r_K^- m_K^+] *recA1 endA1 gyrA96 thi-1 relA1*) cells using a QIAGEN QIAprep® Spin Miniprep kit according to the manufacturer's instructions. Approximate quantity of DNA was determined to be 20 ng·µl^{-1} by gel electrophoresis (1 % agarose, 1 % TAE, 100 V, 20 min.) and comparison to the Promega 1 kb ladder. The plasmid was then digested for 4 hrs at 37 ˚C with the restriction endonuclease *Bam*H I (Fisher, 10 u·µl^{-1}, Table 4.1) using the following mixture: 23 µl pUC19, 3 µl 10x buffer E, 3 µl 10x bovine serum albumin (BSA), and 1 µl *Bam*H I. The cut vector was precipitated with 0.1x volume 3 M sodium acetate, pH 5.2 and 2x volume 95 % ethanol, incubated overnight at –20 ˚C, centrifuged at maximum speed for 30 min. at 4 ˚C, and the supernatant was removed. The pellet was washed twice with 70 % ethanol and allowed to air dry for about 15 min until clear. The DNA was resuspended in 12 µl of 10 mM Tris·HCl, pH 8.0. To dephosphorylate the ends of the cut vector, 1.5 µl calf intestinal alkaline phosphatase (Fisher, 1 u·µl^{-1}) and 1.5 µl 10x alkaline phosphatase buffer was added to 12 µl of the cut vector resuspension and incubated at 37 ˚C for 1 hr. To heat inactivate the phosphatase, the mixture was incubated at 65 ˚C for 15 - 20 min.

To remove any vector with phosphorylated ends, the vector was allowed to self-ligate by adding 2.5 µl dH_20, 2 µl 10x ligase buffer, and 0.5 µl T4 ligase (Fisher, 3 u·µl^{-1}) to 15 µl of the dephosphorylated cut vector mixture. The ligation mixture was incubated at 4 ˚C overnight. The

linearized vector was purified from the religated vector by gel electrophoresis [1 % low melt point agarose (FisherBiotech), 1x TAE, 60 V, 12 hrs]. To avoid induced mutations from ethidium bromide or ultraviolet (UV) light, the edge of the agarose gel was cut to remove the ladder and a sliver of the lane containing the ligation mixture. The gel fragment was stained with ethidium bromide for visualization under UV light. The linearized pUC19 plasmid vector was cut from the unstained gel at approximately 2.7 kb and extracted from the gel using the QIAGEN QIAquick® Gel Extraction kit according to the manufacturer's instructions (30 µl final volume).

Table 4.1. Restriction endonucleases, restriction sites, and DNA digested.

Endonuclease	Restriction Sites*	DNA Digested
***Sau*3A I**	**5'…GATC…3'** **3'…CTAG…5'**	Genomic DNA
***Bam*H I**	**5'…GGATCC…3'** **3'…CCTAGG…5'**	pUC19 vector
***Pvu* II**	**5'…CAGCTG…3'** **3'…GTCGAC…5'**	Genomic library clones

* Arrows indicate the enzyme restriction sites.

To test that the linearized vector was purified from any religated vector, 1 µl of the purified linearized vector and 1 µl of the uncut vector were each added to 40 µl of electrocompetent *E. coli* DH5α cells and electroporated with a BioRad GENE Pulser (25 µF, 200 ohms, and 25 $V \cdot s^{-1}$). Immediately following electroporation, 1 ml of SOC media was added to the cells and incubated at 37 ˚C for 45 min with occasional, gentle agitation. Cell suspension aliquots of 100 µl were plated from each electroporation on LBA + 50 $\mu g \cdot ml^{-1}$ ampicillin (AMP), and 100-µl aliquots of 10^{-1} dilutions of the cell suspensions were plated on LBA, and all plates were incubated overnight at 37 ˚C. No colonies were present on LBA + AMP from the culture transformed with cut vector, and colonies were present on all other plates, indicating that the purified cut vector was not contaminated with uncut or religated vector.

Genomic DNA Preparation

Genomic DNA extraction from *C. ilecola* was modified from Harwood and Cutting, 1990 as described in Chapter 3. The extracted genomic DNA was partially digested with *Sau*3A I (Fisher, 10 $u \cdot \mu l^{-1}$) to produce DNA segments of 2.5 – 5.0 kb. *Sau*3A I was the chosen restriction endonuclease for two reasons. First, it is a four-nucleotide base pair-cutting enzyme, and therefore is expected to cut frequently throughout the genome. Second, the *Sau*3A I cut site is compatible with the *Bam*H I cut site, which is one of the restriction sites within the multiple cloning site on the chosen vector, pUC19 (Table 4.1). Test digests were performed to determine the appropriate *Sau*3A I concentration and incubation time to produce the desired DNA segment sizes, 2.5 -5.0 kb (Figure 4.1 A). Test digests were prepared with 0, 0.005, 0.01, 0.05, 0.1, or 0.5 u *Sau*3A I, 2 µl genomic DNA, 1 µl 10x BSA, 1 µl 10x buffer B, and water to bring the volume to 10 µl total. Digestion mixtures were spilt into two tubes, one set was incubated at 37 ˚C for 15

min and the other set was incubated at 37 ˚C for 30 min. Both sets were heat inactivated for 15 min at 65 ˚C immediately following incubation. Digests were visualized by gel electrophoresis (0.8 % agarose, 1x TAE, 80 V, 1 hr) and ethidium bromide staining (Figure 4.1 A).

The reaction mixture containing 0.05 u *Sau*3A I and incubated for 30 min at 37 ˚C produced the desired DNA segment sizes (Figure 4.1 B). Of the original genomic DNA extraction, 40 µl was digested as described with 0.05 u *Sau*3A I, without scaling up the final reaction volume. The partially digested genomic DNA was visualized by gel electrophoresis [1 % low melt point agarose, 1x TAE, 80 V, 1 hr]. A sliver of the gel containing the genomic DNA was removed with the 1 kb ladder (Promega), stained with ethidium bromide, and visualized under ultraviolet light to check the size of the partially digested DNA. A smear of DNA ranging from above 10 kb to below 0.25 kb was clearly visible (Figure 4.1 B). Although the DNA was not as well digested as in the test digest, DNA segments ranging from 2.5 – 5.0 kb were present in the smear. These segments were cut from the original gel and extracted from the gel using the QIAGEN QIAquick® Gel Extraction kit according to the manufacturer's instructions (50 µl final volume).

Genomic Library Construction

The extracted, genomic DNA segments were ligated into the purified, cut pUC19 vector following a protocol developed in the Handelsman laboratory (Handelsman, unpublished). First, 4 µl pUC19 and 4.5 µl genomic DNA was mixed and heated to 55 ˚C for 2 min. After the DNA mixture returned to room temperature, 1 µl ligase buffer and 0.5 µl T4 DNA ligase (Fisher, 3 $u \cdot \mu l^{-1}$) were added, and the ligation mixture was incubated overnight at 4 ˚C. Transformations were performed as described above except with 2, 3, 4, or 5 µl of the ligation mixture to

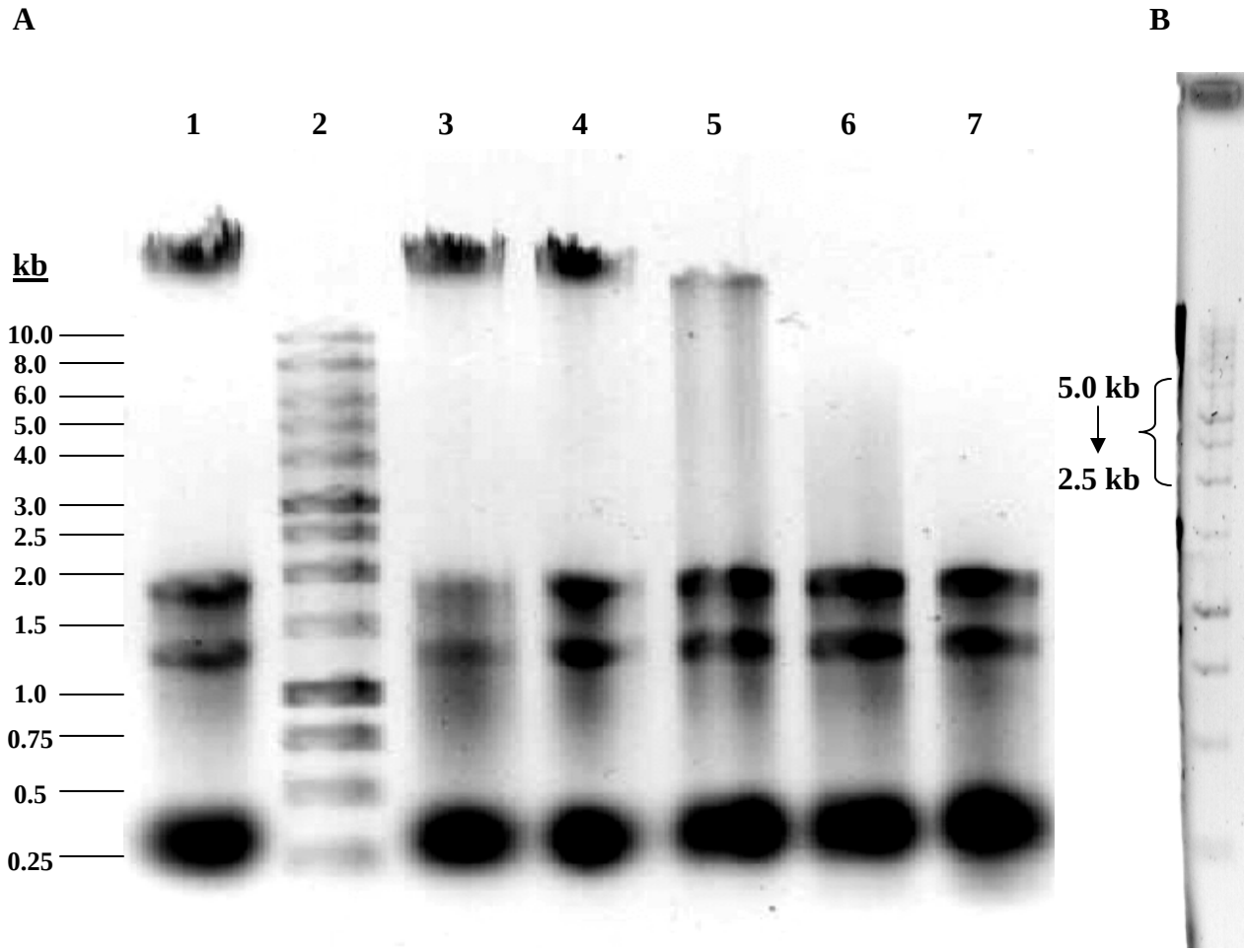

Figure 4.1. Partial digestion of *C. ilecola* genomic DNA with *Sau*3A I. (A) Test digest, lane 1 contains undigested *C. ilecola* genomic DNA. Lane 2 contains 5 µl Promega 1 kb ladder. Lanes 3 – 7 contain *C. ilecola* genomic DNA digested with 0.005, 0.01, 0.05, 0.1, and 0.5 u *Sau*3A I for 30 min. at 37 ˚C. (B) Partially digested *C. ilecola* genomic DNA used in library formation (0.05 u *Sau*3A I for 30 min. at 37 ˚C). Partially digested DNA is visible on the left edge of the gel. Brackets indicate DNA segment sizes (2.5 – 5.0 kb) cut out of unstained gel. Lane on right contains 5 µl Promega 1 kb ladder.

determine which volume would produce the highest transformation efficiency. The most efficient transformation was with 4 µl of the ligation mixture; therefore the remaining digested genomic DNA was ligated and transformed following this protocol. Aliquots of 200 µl transformed cells were plated onto LBA + AMP media and incubated overnight at 37 ˚C. Presence of plasmids was checked for 19 transformants. The transformants were grown in LBA + AMP, plasmids were purified by a modified Qiagen miniprep protocol (Williamson and Allen, unpublished) and digested with 0.5 µl *Pvu* II (Fisher, 10 $u \cdot \mu l^{-1}$), 1 µl 10x buffer B, 1 µl 10x BSA, and 7.5 µl plasmid DNA. Restriction digests were incubated at 37 ˚C for 1 hr, and then analyzed by gel electrophoresis (0.8 % agarose, 1x TAE, 80 V, 45 min).

Library and Individual Clone Storage

For library storage, subpools were made from groups of 400 transformants scraped off LBA + AMP plates. The transformants were added to 100 µl LB + AMP and vortexed to mix. Then 100 µl LB + 33 % glycerol (v/v) + 1.5 x AMP was added to the cell suspension and again vortexed to mix. Aliquots of 80 µl were distributed into three cryovials labeled “subpool ”, and 10 µl aliquots were distributed into four cryovials labeled “master mix.” The subpools contain the separate groups of 400 transformants, while the master mixes contained 10 µl from each subpool, which were vortexed well before freezing at –80 ˚C. Individual clones were grown in 5 ml LB + AMP overnight at 37 ˚C, cells were pelleted at 5,000 x g for 10 min, resuspended in 0.9 ml LB + 33 % glycerol (v/v) + 2 x AMP, vortexed to mix well, and stored at –80 ˚C.

Library Screening

While making subpools for library storage, the first 1,200 transformants were also patched onto LBA + AMP plates. These LBA + AMP plates were subsequently used as master plates for screening via replica plating. The *C. ilecola* library was screened on LBA + AMP + 1 $g \cdot L^{-1}$ MUA, MUC, MUG, or MUX. The library was not screened on medium containing MUM since *C. ilecola* is unable to hydrolyze MUM. Fluorescence was determined via exposure to UV light after 24 and 48 hrs of incubation at 37 ˚C in the dark. Transformants positive for MU-conjugated sugar degradation were retested two more times for fluorescence on the same medium. Only transformant cells from LB + AMP plates that were not exposed to UV light were used to inoculate subsequent cultures.

Sequencing of Cloned Inserts

To purify the plasmids for sequencing, all nine transformants were grown in LBA + AMP overnight at 37 ˚C. Plasmids were purified using a QIAGEN QIAprep® Spin Miniprep kit according to the manufacturer's instructions. Sequencing was performed by Core Technology Alliane, Michigan Life Sciences Corridor, Ann Arbor, MI.

Results and Discussion

Library Screening

Nine of the 1,200 screened clones were able to degrade MUG. None of the screened clones detectably cleaved MUA, MUC, or MUX. All 9 transformants contained plasmids with inserts larger than 1 kb (Figure 4.2). Future studies will include screening the complete library on the five MU-conjugated sugars.

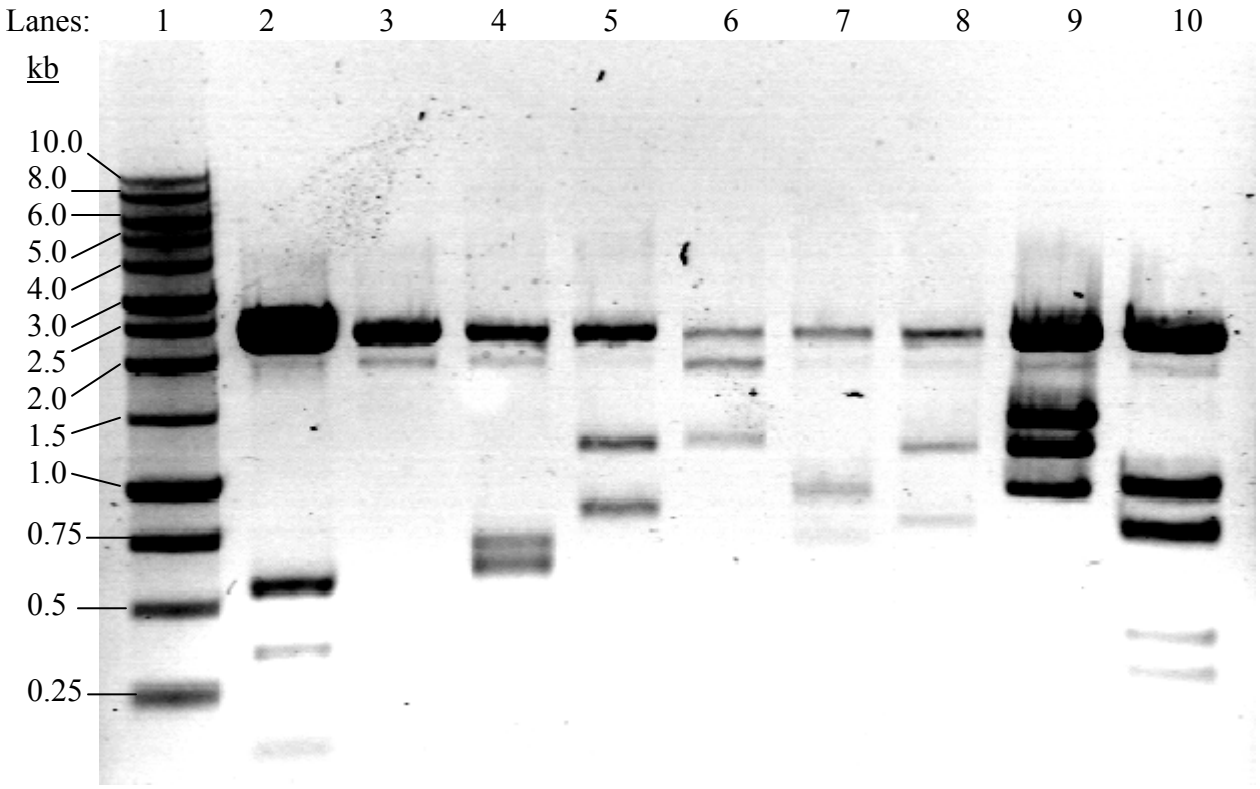

Figure 4.2. Restriction digests of nine *C. ilecola* genomic library clones that demonstrate β-1,4-glucosidase activity. Lane 1 contains 4 µl Promega 1 kb ladder. Lanes 2 – 10 contain genomic library clones 1 – 9, digested with *Pvu* II.

Sequencing of Cloned Inserts

Expression of the cloned insert appeared to be detrimental to the host cells since growth was reduced and both plasmids and inserts were not well maintained relative to transformants containing empty vector (Figure 4.4). Sequencing results have only been obtained for clone numbers 8 and 9, thus far. From the deduced amino acid sequence (EXPASY), clone 8 has 79 % identity and 87 % similarity to the preprotein translocase SecA subunit from *Leifsonia xyli* subsp. *xyli* str. CTCB07 (ncbi locus YP_061618). Clone 9 has 92 % identity and 97 % similarity to

glutamine synthetase from *Leifsonia xyli* subsp. *xyli* str. CTCB07 (ncbi locus YP_061977) from the deduced amino acid sequence.

A genomic library of *C. ilecola* was successfully constructed. Nine transformants demonstrated degradative activity on media containing the model substrate MUG, indicating β-1,4-glucosidase activity. In addition to completing the library screen, the cloned inserts of the seven remaining transformants able to degrade MUG will be sequenced. Future studies will also include the full characterization of the enzymes encoded by the plasmid inserts.

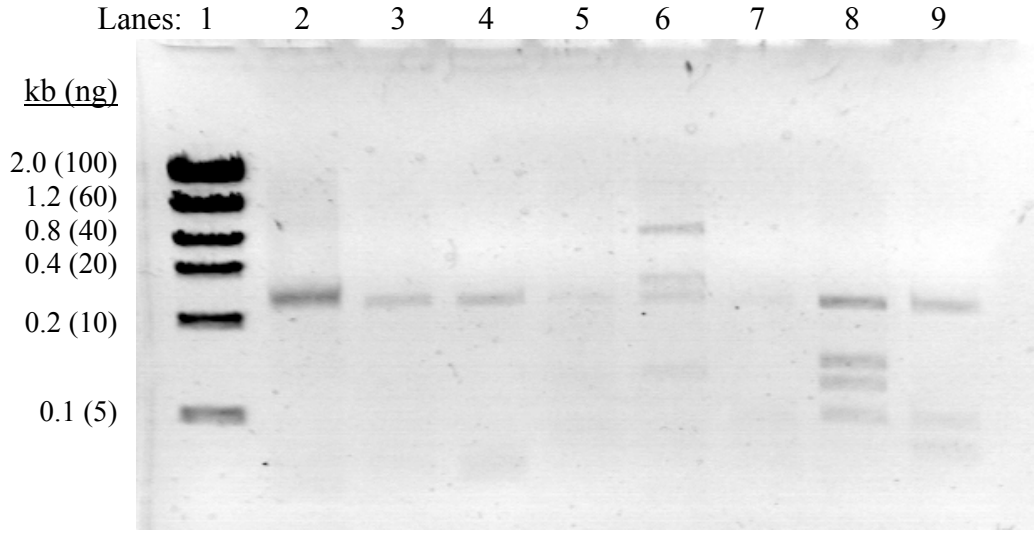

Figure 4.3. Restriction digests of *C. ilecola* genomic library clones purified for sequencing of inserts. Lanes 2 – 9 contain genomic library clones 1 – 6, 8, and 9 digested with *Pvu* II. Lane 1 contains 2 µl Invitrogen Low DNA Mass Ladder.

CHAPTER 5

CONSTRUCTION OF A *TIPULA ABDOMINALIS* HINDGUT METAGENOMIC LIBRARY AND SCREEN FOR LIGNOCELLULASE ACTIVITY

Introduction

Since the majority of microorganisms are as of yet uncultivated, many novel microorganisms and thus novel enzymes will not be found through culturing and screening of isolates alone (Amann et al 1995). Techniques such as cloning and analysis of community 16S rRNA sequences phylogenetically describe microorganisms present within a particular community, but reveal nothing of their metabolic capabilities (Pace et al 1985). Community gene libraries, or metagenomic libraries, are expected to contain all genes in the community (Schloss & Handelsman 2003). Therefore, this technique was chosen to investigate lignocellulose-degrading enzymes from the *T. abdominalis* microbial hindgut community.

Many members of the microbial community residing in the hindgut of the aquatic crane fly *Tipula abdominalis* have yet to be cultivated (Peterson, unpublished). Many isolated bacteria from the *T. abdominalis* hindgut display a wide variety of enzyme activities, including the degradation of lignocellulosic material (Peterson, unpublished). Many uncultured bacteria may also produce lignocellulose-degrading enzymes. In order to understand how the *T. abdominalis* lignocellulosic diet is degraded, lignocellulose-degrading enzymes must be studied from both cultivated and uncultivated bacteria.

A metagenomic library was constructed to screen for all lignocellulases within the *T. abdominalis* hindgut microbial community[2]. To construct this library, pCF430 was the chosen vector because it can hold up to 50 kb DNA inserts, contains the *E. coli araC* regulator and *araBAD* promoter (an L-arabinose-inducible promoter), and can be expressed in a broad range of hosts (Newman & Fuqua 1999).

Methods

Collection and Dissection of Larvae

T. abdominalis larvae were collected and dissected as described in Chapter 2, except collection was in December 2004. Stream parameters were as follows: pH 6.4; dissolved oxygen, 10.5 mg L^{-1}; water temperature, 4.9 ˚C; conductivity, 15.1 µs cm^{-1}; turbidity, 0.59 NTU; alkalinity, 5.0 mg L^{-1}; <1 mg L^{-1} NO_3^-; and <0.1 mg L^{-1} PO_4^{3-}. After removal of hindguts, each hindgut was weighed then cut with an 18-gauge needle down the middle of the gut to allow for easier removal of microbial cells (Appendix A).

Vector Preparation

The plasmid vector pCF430 (Newman & Fuqua 1999) was previously prepared using the restriction endonuclease *Pst* I (Promega, 10 u·µl^{-1}) to linearize the plasmid (Allen, personal communication).

[2] This metagenomic library was constructed in the laboratory of Dr. Jo Handelsman at the University of Wisconsin-Madison under the guidance of Lynn Williamson. This lab has already been very successful in the construction and analysis of metagenomic libraries (Rondon et al. 1999; Schloss and Handelsman 2003)

Metagenomic DNA Preparation

Metagenomic DNA was extracted from a *T. abdominalis* hindgut following modified protocols from (Broderick et al 2004) and (Rondon et al 1999). Briefly, dissected hindguts and 600 µl BSS were placed in a 1.5 ml centrifuge tube and sonicated for 30 sec in a Branson 2210 ultrasonic bath (50 – 60 Hz, 117 V, 1.0 A; Branson Ultrasonics, Danbury, Conn.). The hindgut was allowed to settle to the bottom of the tube, and 537 µl of the supernatant was removed, placed into a new 1.5 ml tube, and sonicated for an additional 45 sec to lyse cells. To the sonicated supernatant, 60 µl 10 % SDS and 3 µl 50 mg·µl^{-1} proteinase K was added. The tube was gently mixed and incubated at 37 ˚C for 1.5 hr. The salt concentration was increased by the addition of 100 µl 5 M NaCl in order to prevent the hexadecyltrimethyl ammonium bromide (CTAB, added in the next step) from complexing with the DNA.[3] CTAB (80 µl) was added as a 10 % solution in 0.7 M NaCl, mixed, and incubated at 65 ˚C for 30 min. A phenol:chloroform:isoamyl (25:24:1) extraction was performed followed by a chloroform:isoamyl alcohol (24:1) extraction. An ethanol precipitation was performed to concentrate the DNA, and the DNA pellet was resuspended in 50 µl 10 mM Tris·HCl, 1 mM EDTA, pH 8.0 (TE).

Since the DNA suspension was still brown from contaminants such as remaining humic compounds, the DNA was purified by gel electrophoresis (1 % low melt agarose, 1 x TAE, 25 V, overnight) using the QIAGEN QIAEX II Gel Extraction kit following the manufacture's directions (60 µl final volume). The approximate DNA concentration (5 ng·µl^{-1}) was determined by comparison to the Promega 1 kb ladder on an agarose gel.

[3] At NaCl concentrations above 0.5 M, CTAB will complex with cell debris such as cell wall materials, proteins, and polysaccharides to form a precipitate. At concentrations below 0.5 M NaCl, CTAB will complex with DNA to form a precipitate.

The extracted metagenomic DNA was partially digested with *Pst* I (Promega, 10 u·µl^{-1}) to produce DNA segments greater than 20 kb. Digestion was performed with *Pst* I because plasmid pCF430 was also cut with *Pst* I. Also, this enzyme cuts a six base pair palindrome, so it will not cut too often, allowing the DNA segments to remain large. Test digests were performed to determine the appropriate concentration of *Pst* I that will produce DNA segment sizes above 20 kb (Figure 5.1). Test digests were prepared with 0, 5, and 10 u *Pst* I, 2 µl metagenomic DNA, 0.5 µl 10x BSA, 0.5 µl 10x buffer H, and water to bring the volume to 5 µl total. Digest reactions were incubated in a 37 ˚C waterbath for 1 hr. Digests were analyzed by pulsed field gel electrophoresis (PFGE) (gel: 1 % agarose, 1x TAE; 3.5 hr protocol: 0.5x TAE, 14 ˚C, 9 V·min^{-1}, 3 sec initial switch, 5 sec final switch, 100˚ included angle). DNA was visualized with ethidium bromide (Figure 5.1).

The reaction mixture containing 10 u *Pst* I produced slightly larger DNA segments than desired (Figure 5.2). The remaining metagenomic DNA was digested with 12 u *Pst* I, without scaling up the reaction, to produce slightly smaller DNA segments than in the test digest. The partial digests were run on an agarose "sizing" gel to separate the DNA greater than 20 kb from any smaller segments (1 % low melt agarose, 1x TAE, 25 V, 4 ˚C, overnight). DNA was visualized by removing a sliver of the partially digested DNA and the 1 kb ladder (Promega), staining with ethidium bromide, and visualizing under UV light. DNA segments greater than 10 kb were divided into upper and lower sections for gel purification using AgarACE® (Promega) following the manufacturer's instructions (100 µl final volume) (Figure 5.2).

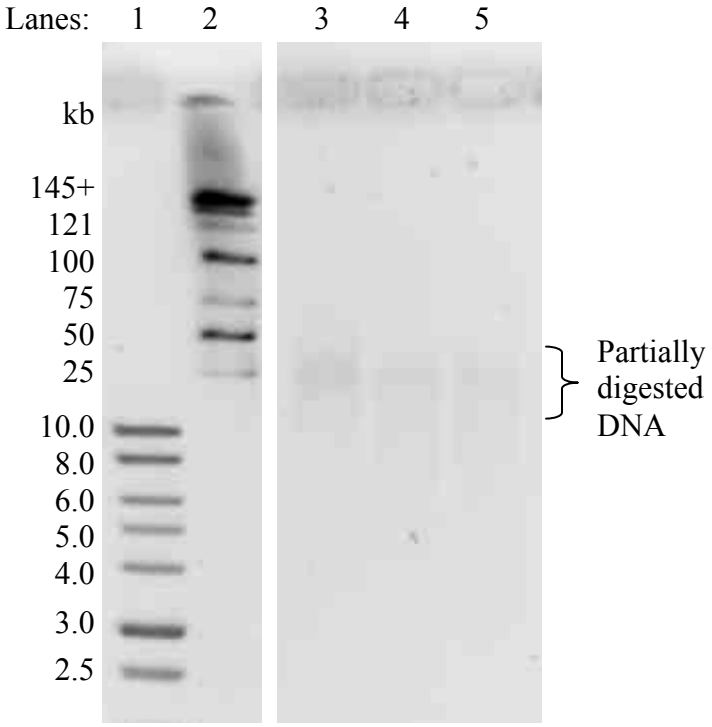

Figure 5.1. Pulsed field gel of metagenomic DNA partial digests. Metagenomic DNA extracted from hindgut homogenates of *T. abdominalis* (2 µl) was digested with 0, 5, and 10 u *Pst* I (lanes 3, 4, and 5, respectively). Lanes 1 and 2 contain 4 µl Promega 1 kb ladder and a sliver of NEB MidRange PFG marker.

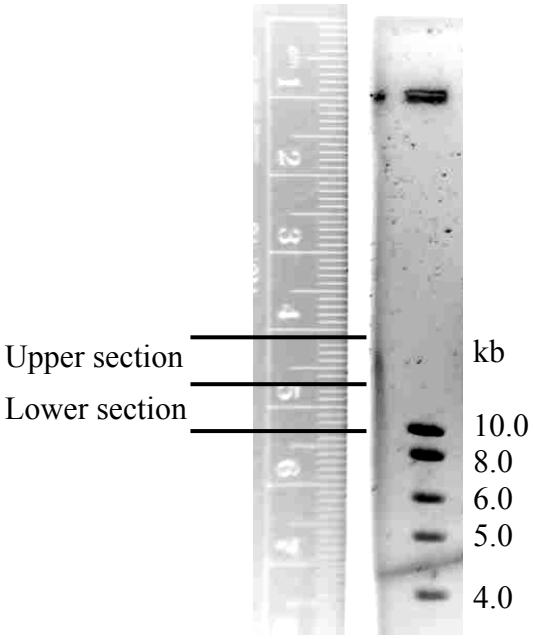

Figure 5.2. Sizing gel of partially digested metagenomic DNA. Metagenomic DNA on left side of sizing gel was digested with 12 u *Pst* I for 1 h at 37 °C. Lane contains 4 µl Promega 1 kb ladder. Upper and lower sections were cut and removed from the unstained gel where indicated.

Metagenomic Library Construction

Separate ligations were prepared for the purified DNA from the upper and lower sections of DNA greater than 20 kb. First, 1 µl vector and 87 µl DNA (concentration of vector DNA was roughly 10 fold greater than insert DNA) were gently mixed and heated to 55 ˚C for 2 min. Then 10 µl ligase buffer and 2 µl T4 DNA ligase (Fisher, 3 u·µl^{-1}) were added, very gently mixed by rolling tube between fingers, and incubated at 4 ˚C overnight. Ligations were desalted on 0.025 µm nitrocellulose filters (Milipore) floated on distilled water for 45 min before transformation by electroporation with TransferMax^{TM} EPI300^{TM} Electrocompetent *E. coli* (Epicentre, cat. No. EC300110). The desalted ligation mixture (5 µl) and *E. coli* cells (45 µl) were mixed then added

to a 0.2 cm elecroporation cuvette for transformation using a BioRad GENE Pulser (25 μF, 200 ohms, 2.5 $V \cdot sec^{-1}$). Immediately following electroporation, cells were suspended in 1 ml SOC medium and incubated at 37 ˚C for 45 min with gentle shaking. Aliquots of 100 μl and 200 μl transformed cells were plated onto two LBA + 20 $\mu g \cdot \mu l^{-1}$ tetracycline (Tet^{20}) and incubated overnight at 37 ˚C. The remaining transformed cell suspension was stored at 4 ˚C overnight.

Of the upper and lower section of DNA greater than 20 kb, only the DNA from the lower section was successfully ligated and transformed. To determine plasmid insert size, isolated transformants were grown in 1.5 ml LB + Tet^{20} at 37 ˚C overnight and plasmids were purified the following morning (Allen, unpublished). Purified plasmids were digested with *Pst* I to separate the insert from the vector (7 μl DNA, 1 μl 10x BSA, 1 μl 10x buffer, 1 μl *Pst* I, incubated at 37 ˚C for 1 hr). PFGE was performed using the 3.5 hr protocol discussed in the previous section.

Library Storage

Subpools were made by scraping approximately 500 μl of cells off LBA + Tet^{20} plates with a sterile spatula, which were then placed in a 2.0 ml microfuge tube containing 500 μl LB + Tet^{20}. The tube was vortexed for 30 sec to mix well. This was repeated until entire library had been scraped off the plates and placed into tubes. Master mixes of the library were made by combining 40 μl aliquots of each subpool into a cryovial. A total of 14 master mixes were made. An equal volume of LB + Tet^{30} + 33 % glycerol (v/v) was added to all subpools and master mixes. All tubes were vortexed well to mix. Subpools were divided into 4 cryovials (360 μl each). To achieve an ideal cooling rate, cryovials were frozen in a NALGENE “Mr. Frosty” 1 ˚C freezing container and stored at –80 ˚C.

Library Screening

Since *T. abdominalis* hindgut degradative enzyme activity was highest for the substrate MUG relative to the four other MU-conjugated sugars tested in Chapter 2, the initial screen was for only MUG degrading activity. To revive transformants, 1.0 µl of master pool #1 was added to 0.999 ml LB, mixed gently, then diluted 10 fold further with 9.0 ml LB, 100 µl was spread-plated onto LBA + Tet^{20} for a final dilution of 10^{-5}, and incubated at 37 ˚C overnight. Transformants were screened as described in Chapter 4, except L-arabinose was added to the media. The chosen concentration for the screen of the *T. abdominalis* metagenomic library was 50 mM L-arabinose since in a previous study, *lacZ* expression was high when L-arabinose concentrations were between 10 to 100 mM.

Results and Discussion

Metagenomic Library

Plasmids were isolated and digested from 38 transformants to determine insert DNA size. Nineteen of the 38 plasmids had insert DNA larger than ~10 kb (Figure 5.3). Two plasmids appear to have inserts of roughly the same size as the empty vector. Six plasmids contained an insert smaller than the empty vector. One plasmid appeared to be undigested. Six plasmids appeared to be empty, and three plasmids were undetected (Figure 5.3).

Library Screening

Approximately 7,500 transformants were screened on LBA + MUG + 50 mM L-arabinose. No transformants demonstrated activity for degrading MUG. Future studies will include screening the library on media containing various concentrations of L-arabinose to

optimize insert expression. Once the screen is optimized for detection of MUG hydrolysis, the entire library will also be screened on media containing MUA, MUC, MUG, MUX, and various polymeric sugars such as CMC, starch, and xylan.

A metagenomic library with DNA insert sizes between 4 and 40 kb was successfully constructed from a *T. abdominalis* hindgut homogenate. Screening of the library for hydrolysis of MUG was unsuccessful, and future studies will attempt to optimize the screen. Future studies will also include sequencing of inserts to determine if the library is contaminated with insect or plant DNA, and to determine which microorganisms reside within the *T. abdominalis* hindgut and what metabolic capabilities these microorganisms possess.

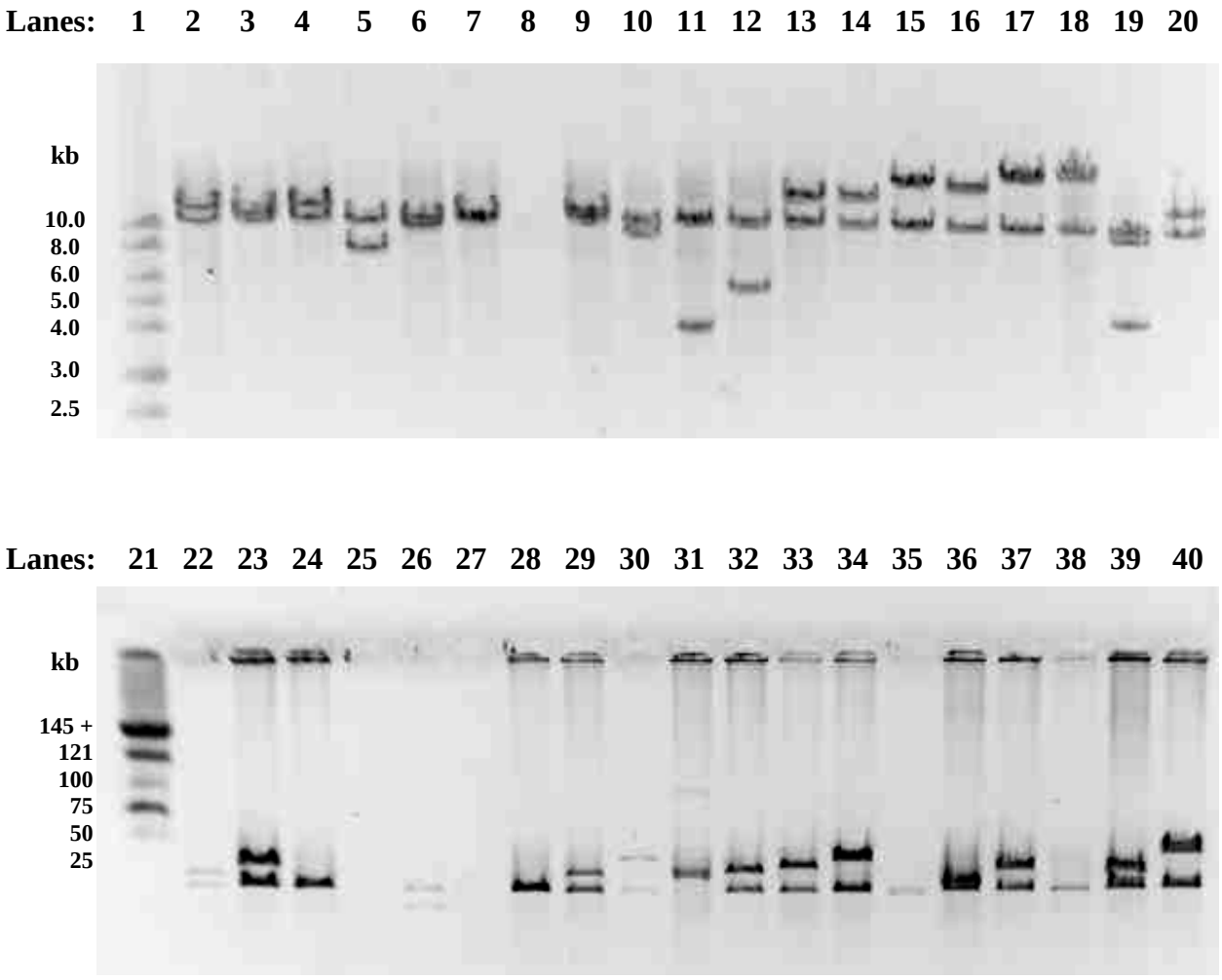

Figure 5.3. Metagenomic library clones from a *T. abdominalis* larval hindgut homogenate. Lanes 1 and 21 contain 5 µl of Promega 1 kb ladder and a sliver of NEB MidRange PFG marker, respectively. Lanes 2 – 20 and 22 – 40 contain metagenomic library clones digested with *Pst* I. Most inserts are 10 kb or larger.

CHAPTER 6

CONCLUSIONS

The main objectives of this study were as follows: (1) to demonstrate cellulolytic and hemicellulolytic activity from fresh *T. abdominalis* gut extracts at a physiologically relevant pH, (2) to culture novel and previously isolated bacteria from the *T. abdominalis* hindgut, and (3) to discover novel cellulases and hemicellulases from the microbial symbionts of the *T. abdominalis* hindgut. Cellulolytic and hemicellulolytic enzyme activity was successfully demonstrated from *T. abdominalis* hindgut enzyme extracts at a physiologically relevant pH of 7.4 utilizing five MU-conjugated sugars as model substrates. Midgut enzyme extracts displayed activities similar to negative controls. It is likely that the high pH of the midgut, pH 11.0, is inactivating most cellulases and hemicellulases. Since cellulolytic and hemicellulolytic enzyme activity was present from hindgut extracts and not from midgut extracts, the majority of cellulose and hemicellulose degradation occurs in the hindgut. The majority of lignocellulose degradation is expected to occur within the anterior hindgut since it is analogous in structure to the termite paunch, where fermentation is facilitated by retarding the passage of food through the hindgut (Klug and Kotarski 1980; Martin, 1987). To test this hypothesis, future studies will include analyzing cellulolytic and hemicellulolytic enzyme activity of the anterior and posterior hindgut separately.

Bacteria isolated from the hindgut extracts were diverse in colony morphology, and many demonstrated cellulolytic and hemicellulolytic activity. Ten of these isolates resembled a bacterium previously cultivated from the hindguts of many *T. abdominalis* larvae collected from

North Carolina and Michigan. One of these isolates, T202^T, was fully characterized and forms a new genus within the family *Microbacteriaceae*, of the order *Actinomycetales*, of the class *Actinobacteria*. Isolate T202^T was named *Crocebacterium ilecola*, gen, nov., sp. nov. Whether *C. ilecola* or any of the bacteria isolated from the *T. abdominalis* hindgut are major members of the microbial community is still unknown. To determine prevalence of the various isolates within the hindgut, future studies may include fluorescence in situ hybridization.

The discovery of novel cellulases and hemicellulases from the microbial symbionts of the *T. abdominalis* hindgut was attempted by constructing and screening a genomic library from the novel isolate *C. ilecola* and a metagenomic library from hindgut homogenates. Screening of the *C. ilecola* genomic library resulted in the detection of nine clones demonstrating β-1,4-glucosidase activity. Future studies include screening the full *C. ilecola* genomic library on MU-conjugated substrates, and optimizing the metagenomic library screen. Although a metagenomic library will allow for the analysis of all genes present in a microbial community, it will not reveal which of these genes are being expressed. To determine which genes are being expressed, the mRNA present within the community can be analyzed by the construction and screening of a cDNA library.

As members of the microbial community and the enzymes they produce within the *T. abdominalis* alimentary system are identified and characterized, the role of these microorganisms with respect to the degradation of lignocellulose may be elucidated. As in other insects, such as termites and siricid woodwasps, the hindgut microbial community of *T. abdominalis* larvae may be intimately involved in supplying nutrition by degrading the lignocellulose rich detritus ingested by the *T. abdominalis* larvae (Martin 1987b, Martin et al 1980a, Sinsabaugh et al 1985b). Results from the studies presented here support this hypothesis. Cellulose and

hemicellulose degrading enzyme activity demonstrated from hindgut extracts indicate that the degradation of lignocellulose rich detritus is occurring within the larval hindgut where microbial colonization occurs. Many of the bacteria isolated from *T. abdominalis* larval hindgut extracts also demonstrated cellulolytic and hemicellulolytic activity. Further studies to determine insect dependence on microbial symbionts of the gut may include axenic rearing or treatment of larvae with antimicrobials. *T. abdominalis* larvae are major shredders of detritus in small order stream ecosystems, and are therefore an important component of carbon and energy cycling within this ecosystem. If the microbial hindgut symbionts of *T. abdominalis* larvae are responsible for the degradation of the ingested detritus, then this microbial community plays an important role in carbon and energy cycling within small order stream ecosystems.

LITERATURE CITED

2003a. Approved standard M2-A7. Performance standards for antimicrobial disk suseptibility tests, 8th ed. In *National Committee for Clinical Laboratory Standards*. Wayne, PA

2003b. *Difco & BBL manual*. Sparks, MD: Becton, Dickinson and Company

Amann RI, Ludwig W, Schleifer K-H. 1995. Phylogenetic identification and insitu detection of individual microbial cells without cultivation. *Microbiol. Rev.* 59: 143-69

Ayers LW. 2000. Textbook of Diagnostic Microbiology. ed. CR Mahon, G Manuselis, pp. 267-8. Philadelphia, PA: W. B. Saunders Company

Barlocher F, Porter CW. 1986. Digestive enzymes and feeding strategies of three stream invertebrates. *J. N. Am. Benthol. Soc.* 5: 58-66

Bayer EA, Belaich JP, Shoham Y, Lamed R. 2004. The cellulosomes: multienzyme machines for degradation of plant cell wall polysaccharides. *Annu Rev Microbiol* 58: 521-54

Behrendt U, Ulrich A, Schumann P, Naumann D, Suzuki K. 2002. Diversity of grass-associated *Microbacteriaceae* isolated from the phyllosphere and litter layer after mulching the sward; polyphasic characterization of *Subtercola pratensis* sp. nov., *Curtobacterium herbarum* sp. nov. and *Plantibacter flavus* gen. nov., sp. nov. *Int J Syst Evol Microbiol* 52: 1441-54

Bjarnov N. 1972. Carbohydrases in *Chironomus*, *Gamarus*, and some Trichoptera larvae. *Oikos* 23: 261-3

Brendelberger H. 1997. Determination of digestive enzyme kinetics: a new method to define trophic niches in freshwater snails. *Oecologia* 109: 34-40

Breznak JA, Brune A. 1994. Role of microorganisms in the digestion of lignocellulose. *Annu. Rev. Entomol.* 39: 453-87

Broderick NA, Raffa KF, Goodman RM, Handelsman J. 2004. Census of the bacterial community of the gypsy moth larval midgut by using culturing and culture-independent methods. *Appl. Environ. Microbiol.* 70: 293-300

Cashion P, Holder-Franklin MA, McCully J, Franklin M. 1977. A rapid method for the base ratio determination of bacterial DNA. *Anal Biochem* 81: 461-6

Cummins KW. 1974. Structure and function of stream ecosystems. *BioSci.* 24: 631-41

Cummins KW, Klug MJ. 1979. Feeding ecology of stream invertebrates. *Ann. Rev. Ecol. Syst.* 10: 147-72

Cummins KW, Petersen RC, Howard FO, Wuycheck JC, Holt VI. 1973. The utilization of leaf litter by stream detritivores. *Ecol.* 54: 336-44

Delalibera I, Jr., Handelsman J, Raffa KF. 2005. Contrasts in the cellulolytic activities of gut microorganisms between the woodborer, *Saperda vestita* (Coleoptera: Cerambycidae), and the bark beetles, *Ips pini* and *Dendroctonus frontalis* (Coleoptera: Curculionidae). *Environ Microbiol* 34: 541-7

Dillon RJ, Dillon VM. 2004. The gut bacteria of insects: nonpathogenic interactions. *Annu. Rev. Entomol.* 49: 71-92

Doetsch RN. 1981. Determinative methods of light microscopy. In *Manual of methods for general microbiology*, ed. P Gerhardt, RGE Murray, RN Costilow, EW Nester, WA Wood, et al, pp. 21-33. Washington, D.C.: American Society for Microbiology

Doi RH, Kosugi A, Murashima K, Tamaru Y, Han SO. 2003. Cellulosomes from mesophilic bacteria. *J Bacteriol* 185: 5907-14

Dorofeeva LV, Evtushenko LI, Krausova VI, Karpov AV, Subbotin SA, Tiedje JM. 2002. *Rathayibacter caricis* sp. nov. and *Rathayibacter festuca*e sp. nov., isolated from the phyllosphere of *Carex* sp. and the leaf gall induced by the nematode *Anguina graminis* on *Festuca rubra* L., respectively. *Int J Syst Evol Microbiol* 52: 1917-23

Dorofeeva LV, Krausova VI, Evtushenko LI, Tiedje JM. 2003. *Agromyces albus* sp. nov., isolated from a plant (*Androsace* sp.). *Int J Syst Evol Microbiol* 53: 1435-8

Enari T-M. 1983. Microbial Cellulases. In *Microbial Enzymes and Biotechnology*, ed. WM Fogarty. London and N.Y.: Applied Science Publishers

Evtushenko LI, Dorofeeva LV, Dobrovolskaya TG, Streshinskaya GM, Subbotin SA, Tiedje JM. 2001. *Agreia bicolorata* gen. nov., sp. nov., to accommodate actinobacteria isolated from narrow reed grass infected by the nematode *Heteroanguina graminophila*. *Int J Syst Evol Microbiol* 51: 2073-9

Evtushenko LI, Dorofeeva LV, Krausova VI, Gavrish EY, Yashina SG, Takeuchi M. 2002. *Okibacterium fritillariae* gen. nov., sp. nov., a novel genus of the family *Microbacteriaceae*. *Int J Syst Evol Microbiol* 52: 987-93

Evtushenko LI, Dorofeeva LV, Subbotin SA, Cole JR, Tiedje JM. 2000. *Leifsonia poae* gen. nov., sp. nov., isolated from nematode galls on *Poa annua*, and reclassification of '*Corynebacterium aquaticum*' Leifson 1962 as *Leifsonia aquatica* (ex Leifson 1962) gen. nov., nom. rev., comb. nov. and *Clavibacter xyli* Davis et al. 1984 with two subspecies as

Leifsonia xyli (Davis et al. 1984) gen. nov., comb. nov. *Int J Syst Evol Microbiol* 50 Pt 1: 371-80

Friedrich U, Prior K, Altendorf K, Lipski A. 2002. High bacterial diversity of a waste gas-degrading community in an industrial biofilter as shown by a 16S rDNA clone library. *Environ Microbiol* 4: 721-34

Golladay SW, Webster JR, Benfield EF. 1983. Factors affecting food utilization by a leaf shredding aquatic insect:leaf species and conditioning time. *Holarctic Ecology* 6: 157-62

Graca MAS, Barlocher F. 1998. Proteolytic gut enzymes in *Tipula caloptera* - interaction with phenolics. *Aquatic Insects* 21: 11-8

Groth I, Schumann P, Weiss N, Martin K, Rainey FA. 1996. *Agrococcus jenensis* gen. nov., sp. nov., a new genus of actinomycetes with diaminobutyric acid in the cell wall. *Int J Syst Bacteriol* 46: 234-9

Hoppe HG. 1983. Significance of exoenzymatic activities in the ecology of brackish water: measurement by means of methylumbelliferyl-substrates. *Mar Ecol Prog Ser* 11: 299-308

Kampfer P, Rainey FA, Andersson MA, Nurmiaho Lassila EL, Ulrych U, et al. 2000. *Frigoribacterium faeni* gen. nov., sp. nov., a novel psychrophilic genus of the family *Microbacteriaceae*. *Int J Syst Evol Microbiol* 50 Pt 1: 355-63

Kimura MA. 1980. A simple method for estimating evolutionary rates of base substitutions through comparative studies of nucleotide sequences. *J. Mol. Evol.* 16: 111-20

Klug MJ, Kotarski S. 1980. Bacteria associated with the gut tract of larval stages of the aquatic cranefly *Tipula abdominalis* (Diptera: Tipulidae). *Appl. Environ. Microbiol.* 34: 408-16

Kyun Han S, Nedashkovskaya OI, Mikhailov VV, Bum Kim S, Sook Bae K. 2003. *Salinibacterium amurskyense* gen. nov., sp. nov., a novel genus of the family *Microbacteriaceae* from the marine environment. *Int J Syst Bacteriol* 53: 2061-6

Lawson DL, Klug MJ, Merritt RW. 1984. The influence of the physical, chemical, and microbiological characteristics of decomposing leaves on the growth of the detritivore *Tipula abdominalis* (Diptera: Tipulidae). *Can. J. Zool.* 62: 2339-43

Leadbetter JR, Breznak JA. 1996. Physiological ecology of *Methanobrevibacter cuticularis* sp. nov. and *Methanobrevibacter curvatus* sp. nov., isolated from the hindgut of the termite *Reticulitermes flavipes*. *Appl Environ Microbiol* 62: 3620-31

Lin-Chao S, Chen W-T, Wong T-T. 1992. High copy number of the pUC plasmid results from a Rom/Rop-suppressible point mutation in RNA II. *Mol. Microbiol.* 6: 3385-93

MacFaddin JF. 1985. *Media for Isolation-Cultivation-Identification-Maintenance of Medical Bacteria*. Baltimore, MD: Williams and Wilkins. 600-4 pp.

MacKenzie SL. 1987. Gas chromatographic analysis of amino acids as the *N*-heptafluorobutyryl isobutyl esters. *J. Assoc. Off. Anal. Chem.* 70: 151-60

Maltby L. 1992. Detritus processing. In *The Rivers Handbook*, ed. P Calow, GE Petts, pp. 331-53. Oxford: Blackwell Scientific Publications

Mannisto MK, Schumann P, Rainey FA, Kampfer P, Tsitko I, et al. 2000. *Subtercola boreus* gen. nov., sp. nov. and *Subtercola frigoramans* sp. nov., two new psychrophilic actinobacteria isolated from boreal groundwater. *Int J Syst Evol Microbiol* 50 Pt 5: 1731-9

Martin MM. 1987a. *Invertebrate-Microbial Interactions*. Ithaca, NY: Comstock Publishing Associates. 148 pp.

Martin MM. 1987b. *Invertebrate-microbial interactions: ingested fungal enzymes in arthropod biology*. Ithaca, NY: Cornell University Press

Martin MM, Martin JS, Kukor JJ, Merritt RW. 1980a. The digestion of protein and carbohydrate by the stream detritivore, *Tipula abdominalis* (Diptera, Tipulidae). *Oceologia* 46: 360-4

Martin MM, Martin JS, Kukor JJ, Merritt RW. 1980b. The digestion of protein and carbohydrate by the stream detrivore, *Tipula abdominalis* (Diptera, Tipulidae). *Oecologia* 46: 360-4

Martin MM, Martin JS, Kukor JJ, Merritt RW. 1981a. Digestive enzymes of the larvae of three species of caddisflies (Trichoptera). *Insect Biochemistry* 5: 501-5

Martin MM, Martin JS, Kukor JJ, Merritt RW. 1981b. The digestive enzymes of detritus-feeding stonefly nymphs (Plecoptera:Pteronarcidae). *Canadian Journal of Zoology* 59: 1947-51

Mesbah M, Whitman WB. 1989. Measurement of deoxyguanosine/thymidine ratios in complex mixtures by high-performance liquid chromatography for determination of the mole percentage guanine + cytosine of DNA. *J Chromatogr* 479: 297-306

Miki T. 1987. *Protein Eng.* 1: 327-32

Mondou F, Shareck F, Morosoli R, Kluepfel D. 1986. Cloning of the xylanase gene of *Streptomyces lividans*. *Gene* 49: 323-30

Monk DC. 1976. The distribution of cellulose and dietary components and pH of the gut in the amphipod, *Gammarus pulex* (L.). *Freshwater Biology* 7: 431-40

Mukhopadhyay N, Almasy L, Schroeder M, Mulvihill WP, Weeks DE. 2005. Mega2: data-handling for facilitating genetic linkage and association analyses. *Bioinformatics* 21: 2556-7

Newman JR, Fuqua C. 1999. Broad-host-range expression vectors that carry the L-arabinose-inducible *Escherichia coli araBAD* promoter and the *araC* regulator. *Gene* 227: 197-203

Nicholas KB, Nicholas HBJ, Deerfield DWI. 1997. GeneDoc: Analysis and visualization of genetic variation. *EMBNEW.NEWS* 4: 14

Pace NR, Stahl DA, Lane DJ, Olsen GJ. 1985. Analyzing natural microbial populations by rRNA sequences. *ASM News* 51: 4-12

Petersen RC, Cummins KW. 1974. Leaf processing in a woodland stream. *Freshwater Biol.* 4: 343-68

Petersen RC, Cummins KW, Ward GM. 1989. Microbial and animal processing of detritus in a woodland stream. *Ecol. Monogr.* 59: 21-39

Prichard G. 1983. Biology of Tipulidae. *Ann. Rev. Entomol.* 28: 1-22

Pritchard G, Hall A. 1971. A introduction to the biology of craneflies in a series of abandoned beaver ponds with an account of the life cycle of *Tipula sacra* Alexander (Diptera; Tipulidae). *Can. J. Zool.* 49: 467-82

Rondon MR, August PR, Bettermann AD, Brady SF, Grossman TH, et al. 2000. Cloning the soil metagenome: a strategy for accessing the genetic and functional diversity of uncultured microorganisms. *Appl. Environ. Microbiol.* 66: 2541-7

Rondon MR, Raffel SJ, Goodman RM, Handelsman J. 1999. Toward functional genomics in bacteria: analysis of gene expression in *Escherichia coli* from a bacterial artificial chromosome library of *Bacillus cereus*. *Proc. Natl. Acad. Sci. USA* 96: 6451-5

Saitou N, Imanishi T. 1989. Relative efficiencies of the Fitch-Margoliash, maximum-likelihood, minimum-evolution, and neighbor-joining methods of the phylogenetic tree construction in obtaining the correct tree. *Mol. Biol. Evol.* 6: 514-25

Sasaki J, Chijimatsu M, Suzuki K. 1998. Taxonomic significance of 2,4-diaminobutyric acid isomers in the cell wall peptidoglycan of actinomycetes and reclassification of *Clavibacter toxicus* as *Rathayibacter toxicus* comb. nov. *Int J Syst Bacteriol* 48 Pt 2: 403-10

Schleifer KH. 1985. Analysis of the chemical composition and primary stucture of murein. *Methods Microbiol* 18: 123-56

Schleifer KH, Kandler O. 1972. Peptidoglycan types of bacterial cell walls and their taxonomic implications. *Bacteriol Rev* 36: 407-77

Schloss PD, Handelsman J. 2003. Biotechnological prospects from metagenomics. *Current Opinion in Biotechnology* 14: 303-10

Schulte U, Spanhoff B, Meyer E. 2003. Ingestion and utilization of wood by the larvae of two Trichoptera species, *Lasiocephala basalis* (Lapidostomatidae) and *Lype phaeopa* (Psychomyiidae). *Arch. Hydrobiol.* 158: 169-83

Schumann P, Behrendt U, Ulrich A, Suzuki K. 2003. Reclassification of *Subtercola pratensis* Behrendt et al. 2002 as *Agreia pratensis* comb. nov. *Int J Syst Evol Microbiol* 53: 2041-4

Shallom D, Shoham Y. 2003. Microbial hemicellulases. *Curr Opin Microbiol* 6: 219-28

Sheridan PP, Loveland-Curtze J, Miteva VI, Brenchley JE. 2003. *Rhodoglobus vestalii* gen. nov., sp. nov., a novel psychrophilic organism isolated from an Antarctic Dry Valley lake. *Int J Syst Evol Microbiol* 53: 985-94

Singh J, Batra N, Sobti RC. 2004. Purification and characterization of alkaline cellulase produced by a novel isolate, *Bacillus sphaericus* JS1. *Journal of Industrial Microbiology and Biotechnology* 31: 51-6

Sinsabaugh RL, Benfield EF, Linkins AE. 1981. Cellulase activity associated with the decomposition of leaf litter in a woodland stream. *Oikos* 36: 184-90

Sinsabaugh RL, Linkins AE, Benfield EF. 1985a. Cellulose digestion and assimilation by three leaf-shredding aquatic insects. *Ecology* 66: 1464-71

Sinsabaugh RL, Linkins AE, Benfield EF. 1985b. Cellulose digestion and assimulation by three leaf-shredding aquatic insects. *Ecology* 66: 1464-71

Sreerama L, Veerabhadrappa PS. 1991. Purification and properties of carboxylesterases from the midgut of the termite *Odentotermes horni* W. *Insect Biochem* 21: 833-44

Staneck JL, Roberts GD. 1974. Simplified approach to identification of aerobic actinomycetes by thin-layer chromatography. *Appl Microbiol* 28: 226-31

Suberkropp K, Klug MJ. 1974. Decomposition of deciduous leaf litter in a woodland stream: A scanning electron microscope study. *Microbiol. Ecol.* 1: 96-103

Suberkropp KF, Godshalk GL, Klug MJ. 1976. Changes in the chemical composition of leaves during processing in a woodland stream. *Ecology* 57: 720-7

Tamaoka J, Komagata K. 1984. Determination of DNA base composition by reversed-phase high-performance liquid chromatography. *FEMS Microbiol Lett* 25: 125-8

Tarrand JJ, Groschel DH. 1982. Rapid, modified oxidase test for oxidase-variable bacterial isolates. *J Clin Microbiol* 16: 772-4

Thompson JD, Gibson TJ, Plewniak F, Jeanmougin F, Higgins DG. 1997. The CLUSTAL_X windows interface: Flexible strategies for multiple sequence alighnment aided by quality analysis tools. *Nucleic Acids Res.* 25: 4876-82

Tsukamoto T, Takeuchi M, Shida O, Murata H, Shirata A. 2001. Proposal of *Mycetocola* gen. nov. in the family *Microbacteriaceae* and three new species, *Mycetocola saprophilus* sp. nov., *Mycetocola tolaasinivorans* sp. nov. and *Mycetocola lacteus* sp. nov., isolated from cultivated mushroom, *Pleurotus ostreatus*. *Int J Syst Evol Microbiol* 51: 937-44

Tuchman NC, Wetzel RG, Rier ST, Wahtera KA, Teeri JA. 2002. Elevated atmospheric CO2 lowers leaf litter nutritional quality for stream ecosystem food webs. *Global Change Biology* 8: 163-70

Vera HD, Dumoff M. 1974. Culture Media. In *Manual of Clinical Microbiology*, ed. EH Lennette, EH Spaulding, JP Truant, pp. 881-929. Washington, D.C.: ASM

Visuvanathan S, Moss MT, Stanford JL, Hermon-Taylor J, McFadden JJ. 1989. Simple enzymatic method for isolation of DNA from diverse bacteria. *J. Microbiol. Methods* 10: 59

Wallace JB, Eggert SL, Meyer JS, Webster JR. 1999. Effects of resource limitation on a detrital-based ecosystem. *Ecol. Monogr.* 69: 409-42

Wood WA, Kellogg ST, eds. 1988. *Biomass Part A, Cellulose and Hemicellulose*, Vols. 160. San Diego, CA: Academic Press

Woodcock TS, Huryn AD. 2005. Leaf litter processing and invertebrate assemblages along a pollution gradient in a Maine (USA) headwater stream. *Environ Pollut* 134: 363-75

Yanisch-Perron C, Vieira J, Messing J. 1985. Improved M13 phage cloning vectors and host strains: nucleotide sequences of the M13mp18 and pUC19 vectors. *Gene* 33: 103-19

Zlamala C, Schumann P, Kampfer P, Rossello-Mora R, Lubitz W, Busse HJ. 2002. *Agrococcus baldri* sp. nov., isolated from the air in the 'Virgilkapelle' in Vienna. *Int J Syst Evol Microbiol* 52: 1211-6

APPENDIX A

TIPULA ABDOMINALIS LARVAE USED IN STUDIES

Insect #	Collection Date	Whole Gut Weight (g)*	Midgut Weight (mg)	Hindgut Weight (mg)	Spiracle Diameter (μm)	Chapter/ Appendix
10	3/24/04	1.11	238	147	686	Ch. 2
11	3/24/04	1.36	259	237	587	Ch. 2
12	3/24/04	1.06	262	200	496	Ch. 2
13	3/24/04	0.889	199	159	457	Ch. 2
14	3/24/04	0.848	148	158	663	Ch. 2
15	3/24/04	0.791	265	150	671	Ch. 2
16	3/24/04	0.983	239	167	564	Ch. 2
17	3/24/04	0.898	161	107	496	Ch. 2
18	3/24/04	0.709	134	120	572	Ch. 2
19	3/24/04	1.12	234	149	465	Ch. 2
20	3/24/04	1.18	287	191	691	Ch. 2
21	3/24/04	0.818	169	146	419	Ch. 2
22	12/14/04	0.372	56.0	35.3	76	Ch. 5
23	12/14/04	1.72	355	212	190	Ch. 5
24	12/14/04	0.333	83.3	23.2	200	Ch. 5
25	12/14/04	0.674	136	122	190	Ch. 5
26	12/14/04	0.392	68.2	73.2	240	Ch. 5
27	12/14/04	0.510	92.1	92.0	320	Ch. 5
28	12/14/04	0.357	46.9	71.8	160	Ch. 5
29	12/14/04	0.36	83.9	65.7	343	Ch. 5
30	12/14/04	0.425	79.9	59.4	267	Ch. 5
31	12/14/04	0.347	43.9	35.7	198	Ch. 5
32	12/14/04	0.449	85.6	77.2	114	Ch. 5
33	12/14/04	0.308	57.2	33.9	190	Ch. 5
34	12/14/04	0.267	48.3	45.2	206	Ch. 5
35	12/14/04	0.339	53.5	58.2	175	Ch. 5
36	12/14/04	0.4547	80.2	66.0	160	Ch. 5
37	12/14/04	0.251	52.8	36.6	190	Ch. 5

*All guts were measured by wet weight. See Appendix B for wet to dry gut weight conversion.

APPENDIX B

DRY GUT WEIGHT TO WET GUT WEIGHT COMPARISON

A

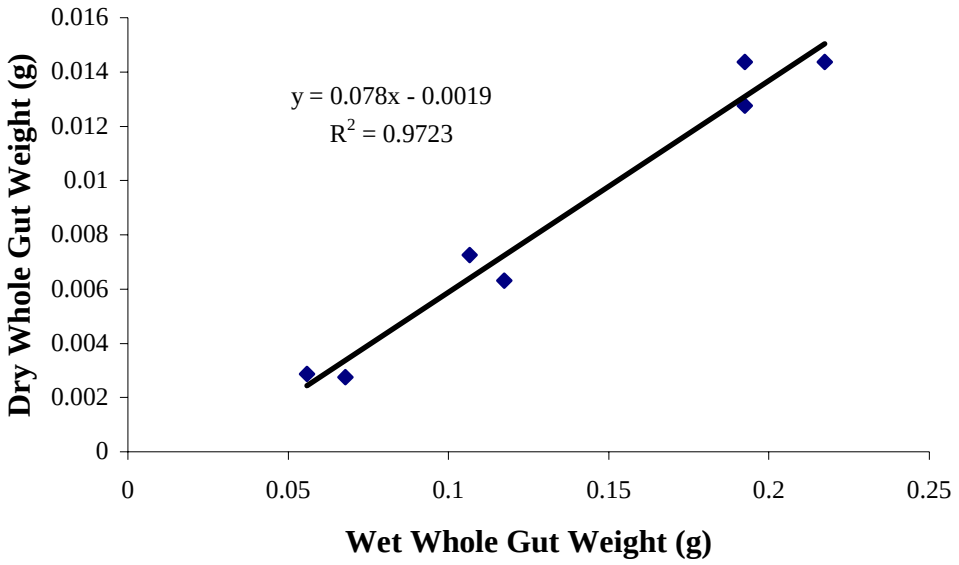

B

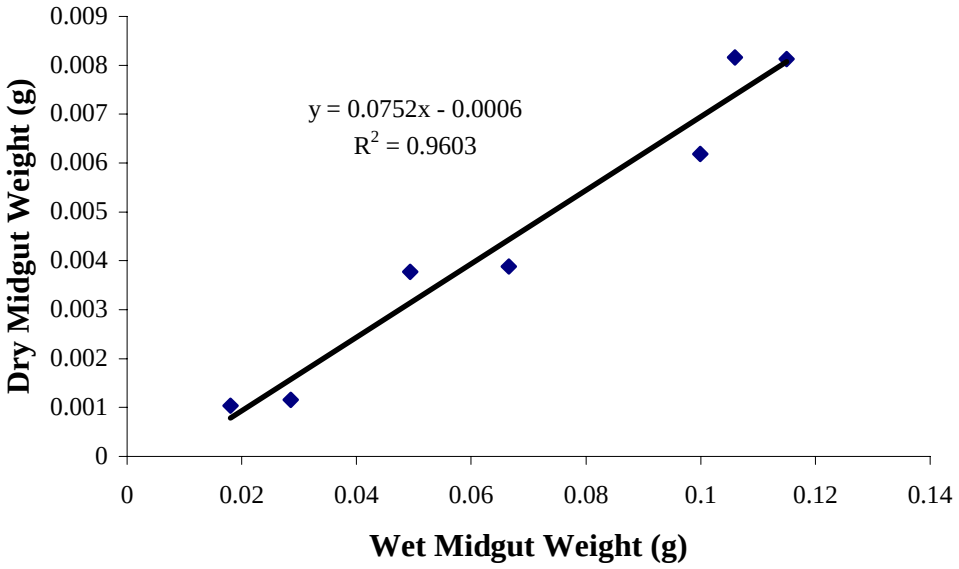

C

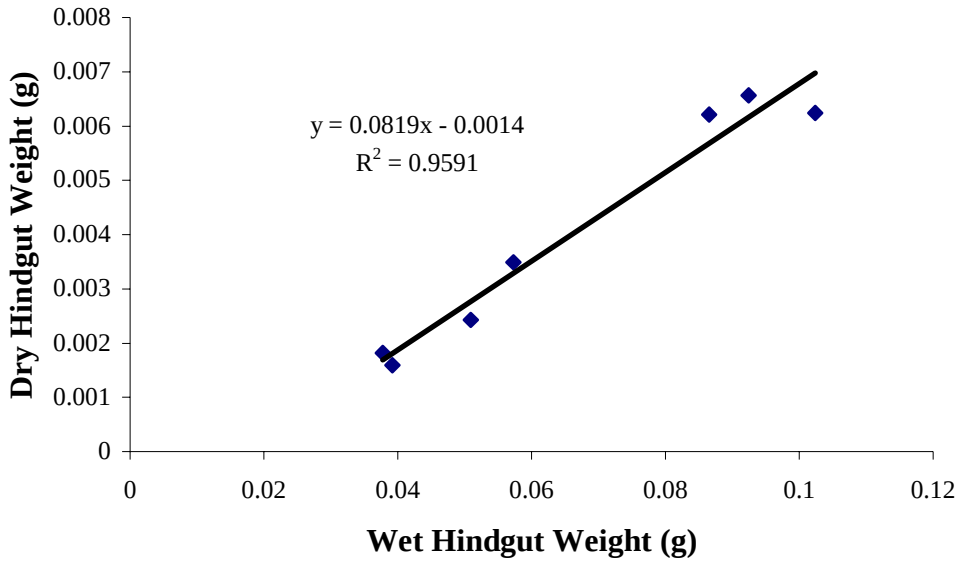

Appendix B. Wet weight vs. dry weight (g) for *T. abdominalis* whole guts (A), midguts (B), and hindguts (C). Dry weight was determined by heating wet gut material at 105 °C for 67 hrs in pre-weighed aluminum weigh boats.